

We are IntechOpen, the world's leading publisher of Open Access books Built by scientists, for scientists

4,800

Open access books available

122,000

International authors and editors

135M

Downloads

Our authors are among the

154

Countries delivered to

TOP 1%

most cited scientists

12.2%

Contributors from top 500 universities



WEB OF SCIENCE™

Selection of our books indexed in the Book Citation Index
in Web of Science™ Core Collection (BKCI)

Interested in publishing with us?
Contact book.department@intechopen.com

Numbers displayed above are based on latest data collected.
For more information visit www.intechopen.com



Cogeneration Power-Desalting Plants Using Gas Turbine Combined Cycle

M.A. Darwish, H.K. Abdulrahim, A.A. Mabrouk and
A.S. Hassan

Additional information is available at the end of the chapter

<http://dx.doi.org/10.5772/60209>

Abstract

The gas-steam turbine combined cycle (GTCC) is the preferred power plant type because of its high efficiency and its use of cheap and clean natural gas as fuel. It is also the preferred type in the Arab Gulf countries where it is used as cogeneration power-desalting plant (CPDP). In this chapter, descriptions and analysis of the GTCC components are presented, namely, the gas turbine cycle (compressor, combustor, gas turbine), heat recovery steam generator, and steam turbine. Combinations of the GTCC with thermally driven desalination units to present CPDP are presented. A parametric study to show the effect of using GTCC on several operating parameters on the CPDP is also presented, as well as cost allocation methods of fuel between the two product utilities (electric power and desalted seawater are also presented).

Keywords: multi stage flash, multi effect with thermal vapor compression, reverse osmosis, steam power plants, gas turbines, combined cycle, cost allocation, energy and exergy analyses

1. Introduction

The efficiency of power plant (PP) using gas turbine (GT) combined cycle (GTCC) is higher than that of steam cycle PP prevailed as baseload-type plant before 2000, and the GT power cycle that was used as peak load and starting units in these steam PPs. The efficiency of the steam turbine (ST) plants is in the range of 35–40 %, the GT is in the range of 30–36 %, and

GTCC is in the range of 45–58 % (Figure 1). This is the main reason for the GTCC to become the preferred-type PP in the Gulf Cooperation Countries (GCC) and worldwide, besides using clean and cheap natural gas (NG) as a fuel. Increasing the PP efficiency reduces the emissions of greenhouse gases (GHG), sulfur dioxide, and nitrogen oxide. The GTCC (Figure 2a) includes an upper GT cycle (i.e., compressor, combustion chamber (cc), gas turbine) and bottom steam cycle (i.e., heat recovery steam generator (HRSG), steam turbine (ST), and condenser). The GT cycle produces almost 2/3 of the GTCC electric power (EP) output, with mainly NG used as fuel supplied to the cc. Hot gases exhausted from the GT (typically at 475–600 °C) are directed to HRSG to produce steam. This steam, when at high-enough temperature and pressure, is directed to ST to produce more work without adding more fuel. The ST cycle produces about 1/3 of the GTCC power output. Processed heat (in the form of steam) produced from the HRSG or extracted (or discharged) from the ST can be used to operate desalting plant (DP), district heating absorption cooling, and/or other processes.

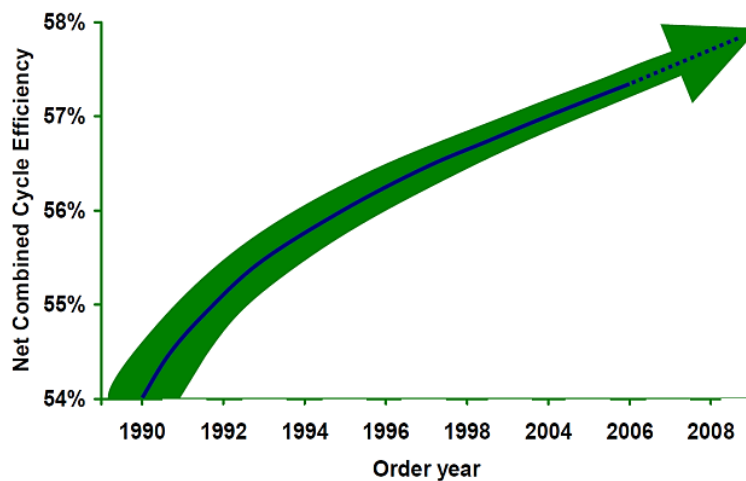


Figure 1. SGT6-5000F CC efficiency evolution [2]

Most PPs in the GCC are cogeneration power-desalting plants producing both desalted seawater (DW) and EP in single plants called CPDP. The desalting units are supplied with its needed low-pressure (LP) steam by extracting (or discharging) steam from the ST of the GTCC or directly from the HRSG when the ST is not operated or does not exist. The ST used in the GTCC can be extraction-condensing steam turbine (ECST) or back-pressure steam turbine (BPST) discharging all of its steam to the DP. Examples of recently installed CPDP using GTCC are Shuaiba North in Kuwait, (Figure 2b), Jebel Ali in the UAE, and Ras Girtas and Mesaieed in Qatar.

In Kuwait, all power plants were of steam type before 2003 and were combined with mainly multistage flash (MSF) desalting plants (DP) up to 2003 to form CPDP; see Table 1. The use of ST for power production in Kuwait followed the 1980s general world trend of using ST in the PP, when the share of GTCC plants was very limited. In the 1990s, the share of GTCC increased very rapidly in the world due to extensive improvements in the GTs. These improvements in GT resulted in reliable GTCC technology and low capital cost of the GTCC plants compared to the ST cycle of the same capacity. NG availability at low cost in many parts of the world and

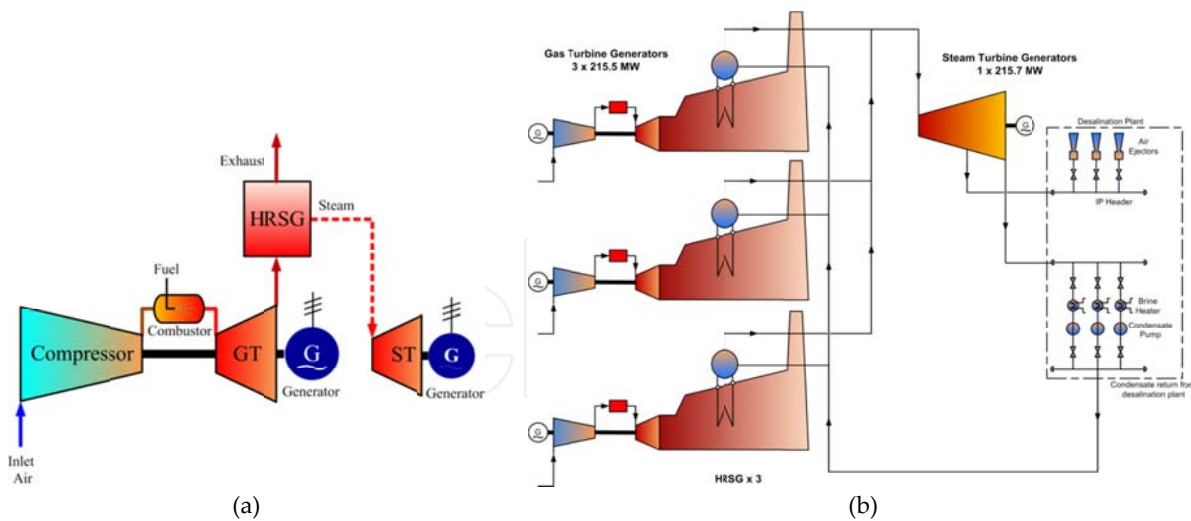


Figure 2. a: Gas turbine combined with steam turbine forming GTCC [1] b: Schematic diagram of Shuaiba North (GTCC) combined with MSF desalination plant

the high efficiency of the GTCC (and thus the use of less fuel with less impact on the environment) promoted the share of the GTCC all over the world. Today, the GTCC-type PP becomes the preferred choice of PPs in most areas in the world, particularly in the GCC as shown in Table 2. Moreover, the GTCC equipment costs are less than that of the conventional ST plants.

Plant name	Date of commissioning	Capacity of steam power plant	Number and size of MSF units
Shuwaikh	1982		3 units × 6.5 MIGD
Shuaiba	1971–1975	6 turbine × 120 MW	6 units × 4.4 MIGD
Doha East	1978–1979	7 turbine × 150 MW	7 units × 6 MIGD
Doha West	1983–1985	8 turbine × 300 MW	4 units × 6 MIGD 12 units × 7.2 MIGD
Az Zour South	1988–2001	8 turbine × 300 MW	16 units × 7.2 MIGD
Sabiya	2003	8 turbine × 300 MW	8 units × 12.5 MIGD

Table 1. Cogeneration steam power-desalination plants in Kuwait up to 2003 [1]

Project	Contractor	Year	Desalination	MIGD	Power plant MW
Al-Fujairah	Doosan	2002	MSF/RO	12.5×5/37.5	GTCC 656
Al-Taweelah A2	Siemens	2001	MSF	12.5×4	GTCC 710
Al-Taweelah B	Siemens	2004	MSF	12.5×6	GTCC 720
Al-Shuweihat S1	Siemens	2002	MSF	17.0×6	GTCC 1500
Umm Al-Nar B	Hanjung	2000	MSF	12.5×5	GTCC 850
Jebel Ali K II	Fisia Itali	2003	MSF	13.5×3	GTCC 880
Shuaiba II	Doosan	2003	MSF	10.0×10	GTCC 500

Table 2. Recent combined cycle plants with MSF units in the United Arab Emirates and Saudi Arabia [1]

Simple GT cycle (Figures 4a–d) consists of a compressor, turbine, and generator usually mounted on single shaft and combustion chamber (cc). When started, the generator is usually operated as a motor to get sufficient rotor speed. Then, the GT is ignited, and power supply to the generator-motor is switched off. The GT accelerates until it reaches its nominal speed, and generator is synchronized and connected to the power grid. The GT is operated at constant speed to keep constant frequency at the generator output. The load changes are compensated by the adjustment of the input fuel flow to the combustor.

Another arrangement (Figures 5a, b) is to put the compressor and portion of the turbine on one shaft while the other part of the turbine and the generator on another shaft. The compressor with the first part of the turbine is called the gas generator (GG); and the GG output is equal to the compressor-consumed power. The other part of the turbine and generator is called the free turbine, which produces the net GT power output and gives more flexibility. Figure 4b shows GE's LM2500 Base aeroderivative gas turbine package that has dual fuel (oil and gas) capability; fast load response; 16-stage axial-flow compressor; annular combustor; two-stage, high-pressure, and single-rotor gas turbine; and highly efficient six-stage power turbine.

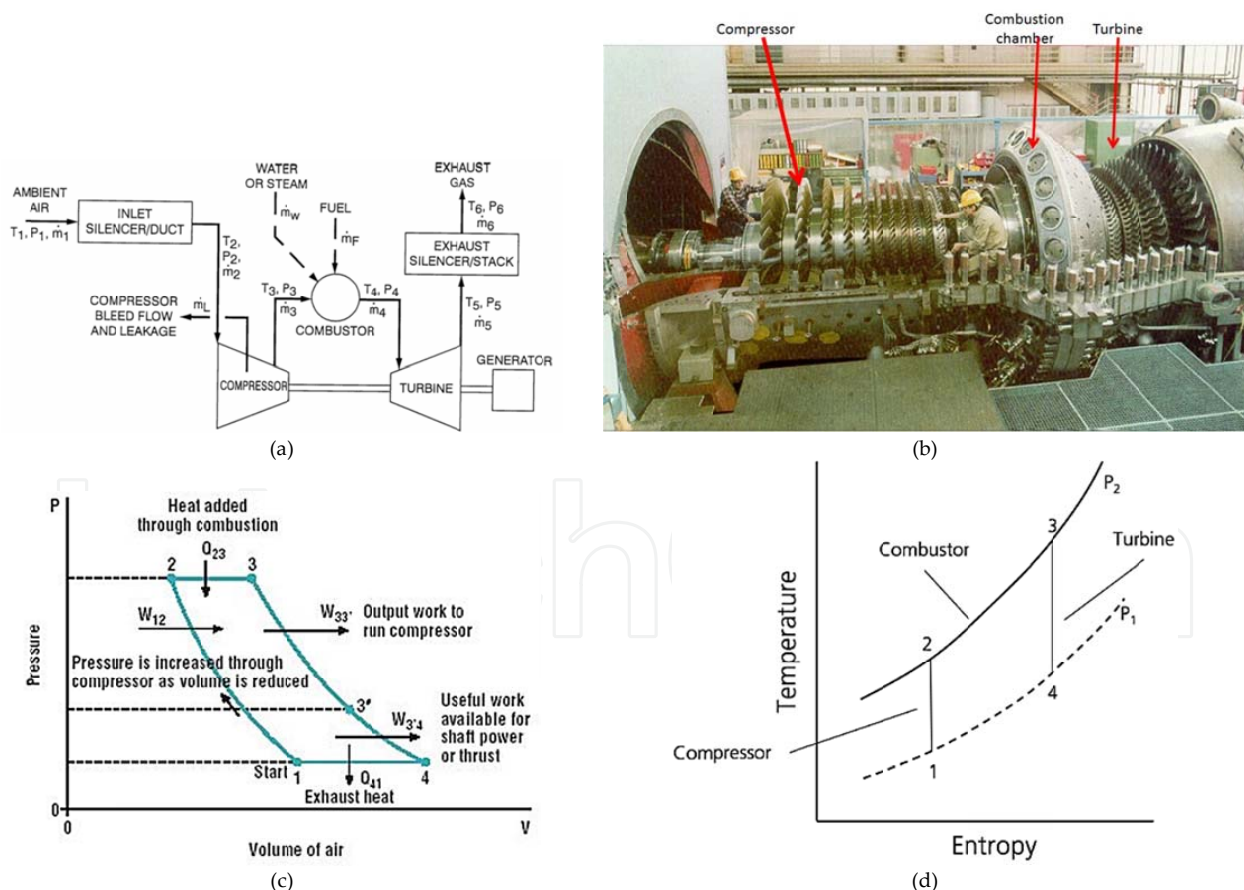


Figure 4. a: Gas turbine open (Brayton) cycle with its operating variables [5] b: Single-shaft gas turbine unit components [5] c: Gas turbine cycle presentation on P-v diagram [5] d: Gas turbine cycle presentation on T-s diagram

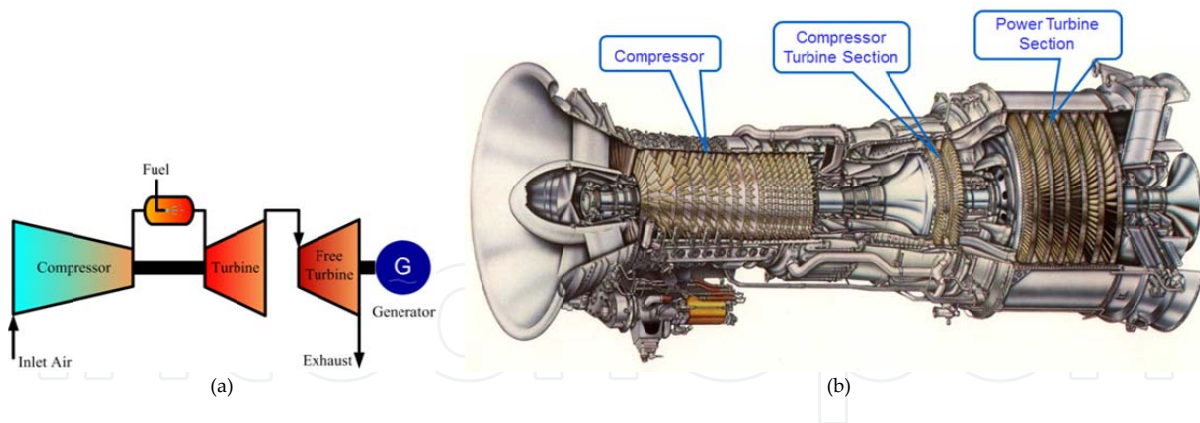


Figure 5. a: Two-shaft GT. b: Two-shaft GE LM2500 aeroderivative GT [6]

2.1. Analysis of ideal gas turbine cycle

The simple ideal gas turbine open cycle (see Figure 4c) known as Brayton cycle consists of four processes:

1. Isentropic compression of ambient air (working fluid) from pressure P_1 to P_2 by a compressor, with $P_2/P_1 = r_p$, called pressure ratio.
2. Heat transfer to the working fluid by mixing fuel with the compressed air and combusted in the cc from 2 to 3; usually P_2 is assumed equal to P_3 for ideal cycle, i.e., isobaric process.
3. Isentropic expansion of the working fluid in GT turbine from 3 to 4.

The exhausted hot gas is released from the turbine to the atmosphere, and fresh air is used to start or continue the cycle. In fact it is not a real cycle, but process 4-1 can be considered as an isobaric process of heat rejection to atmosphere. The cycle can be represented on both pressure-specific volume (P - v) and temperature-entropy (T - s) diagrams as shown in Figure 4d.

When the air is considered as ideal gas, the property relations for process 1-2 are

$$PV = RT, \quad P_1V_1 = RT_1, \quad P_2V_2 = RT_2$$

$$PV^k = C, \quad P_1V_1^k = P_2V_2^k = C$$

where

$$k = C_p / C_v,$$

and then

$$\frac{P_2V_2}{P_1V_1} = \frac{P_2}{P_1} \left(\frac{P_2}{P_1}\right)^{-\frac{1}{k}} = \frac{RT_2}{RT_1}$$

The required compressor-specific process (work per kg) is

$$w_{c, is}(1 \rightarrow 2) = -\int_1^2 v dp = \int_1^2 C \frac{C}{P^{1/k}} dP$$

$$= \frac{k}{1-k} (P_2 v_2 - P_1 v_1) = -\frac{k}{k-1} P_1 v_1 \left(\frac{P_2 v_2}{P_1 v_1} - 1 \right) = -\frac{k}{k-1} R T_1 \left(\frac{P_2}{P_1} \right)^{\frac{k-1}{k}} - 1$$

This is negative work (work consumed by the compressor) and is equal also to

$$|w_{c, is}(1 \rightarrow 2s)| = (h_{2s} - h_1) = c_p (T_{2s} - T_1)$$

T_{2s} and h_{2s} are the absolute temperature and enthalpy at point 2 if the expansion is isentropic ($q_{1-2} = 0$).

Heat addition process from 2 to 3 in the combustion chamber is considered ideal with no pressure loss (isobaric), $P_2 = P_3$. The heat input q_{in} between 2 and 3 is equal to the enthalpy increase: $q_{in} = h_3 - h_{2s} = C_p (T_3 - T_{2s})$.

It is noticed here that T_3 is the highest temperature in the cycle and is called the turbine inlet temperature (TIT). The amount of specific heat input per kg of air is also equal to

$$q_f = \frac{m_f}{m_a} (LHV),$$

where m_f is the mass flow rate of the fuel input and LHV is the fuel low heating value (heat generated per kg of fuel, when the water vapor in the combusted gases is in vapor state).

It is also noticed here that $w_{2-3} = 0$.

The property relations of isentropic expansion process in the turbine can be expressed as

$$PV = RT, \quad P_3 V_3 = RT_3, \quad P_4 V_4 = RT_4$$

$$PV^k = C, \quad P_3 V_3^k = P_4 V_4^k = C$$

The turbine isentropic work is expressed by

$$w_{t, is}(3 \rightarrow 4s) = \int_3^4 v dp = \int_3^4 C \frac{C}{P^{1/k}} dP = \frac{k}{1-k} (P_4 v_4 - P_3 v_3) = -\frac{k}{k-1} P_3 v_3 \left(\frac{P_4 v_4}{P_3 v_3} - 1 \right)$$

$$= \frac{k}{k-1} R T_3 \left(\frac{P_3}{P_4} \right)^{\frac{k-1}{k}} - 1$$

This work can also be expressed by enthalpy change as

$$|w_{t,is}(3 \rightarrow 4s)| = (h_3 - h_{4s}) = c_p(T_3 - T_{4s1})$$

Since part of the turbine work is used to drive the compressor, the net work output ($w_{net} = w_t - w_c$) is expressed as

$$\begin{aligned} w_{net}(ideal) &= w_t - w_c = (h_3 - h_{4s}) - (h_{2s} - h_1) = c_p(T_3 - T_{4s}) - c_p(T_{2s} - T_1) \\ w_{net} &= w_t - w_c = c_p T_3 \left(1 - \frac{T_{4s}}{T_3}\right) - c_p T_1 \left(\frac{T_{2s}}{T_1} - 1\right) \\ &= c_p T_3 \left(1 - \frac{1}{rp^{\frac{k-1}{k}}}\right) - c_p T_1 (rp^{\frac{k-1}{k}} - 1) \end{aligned}$$

It is noticed that the net heat ($q_{in} - q_{out}$) is equal to the net work, or

$$\begin{aligned} \oint \delta Q &= \oint \delta W = q_{in} - q_{out} = w_{out} - w_{in} \\ &= c_p(T_3 - T_{4s}) - c_p(T_{2s} - T_1) = c_p(T_3 - T_{2s}) - q_{out} \\ q_{out} &= c_p(T_{4s} - T_1) = q_{4,1} = c_p \cdot (T_1 - T_4) \end{aligned}$$

The ideal cycle efficiency (net work/heat in) is expressed by

$$\eta = \frac{w_{net}}{q_{in}} = \frac{q_{in} - q_{out}}{q_{in}} = 1 - \frac{q_{out}}{q_{in}} = 1 - \frac{T_{4s} - T_1}{T_3 - T_{2s}} = 1 - \frac{T_1 \left(\frac{T_{4s}}{T_1} - 1\right)}{T_2 \left(\frac{T_3}{T_{2s}} - 1\right)}$$

It is noticed that

$$\begin{aligned} \frac{T_{2s}}{T_1} &= \left(\frac{P_2}{P_1}\right)^{\frac{k-1}{k}}, \quad \frac{T_3}{T_{4s}} = \left(\frac{P_3}{P_4}\right)^{\frac{k-1}{k}}, \quad P_1 = P_4, P_2 = P_3 \\ \frac{T_{2s}}{T_1} &= \frac{T_3}{T_{4s}}, \quad T_{2s} T_{4s} = T_1 T_3, \quad \frac{T_{2s}}{T_3} = \frac{T_1}{T_{4s}}, \end{aligned}$$

Then

$$\eta_c = 1 - \frac{T_1}{T_2} = 1 - \frac{1}{rp^{\frac{k-1}{k}}}$$

where

$$rp = \left(\frac{P_2}{P_1}\right) = \left(\frac{P_3}{P_4}\right)$$

It is noticed that the efficiency depends also on T_3 (TIT), pressure ratio rp , and k , the ratio of specific heats at constant pressure to that at constant volume and is equal to 1.4 for air, $k = \frac{C_p}{C_v}$. The dimensionless work output can be expressed by

$$\frac{w_{net}}{C_p T_1} = \frac{T_3}{T_1} \left(1 - \frac{T_{4s}}{T_3}\right) - \left(\frac{T_2}{T_1} - 1\right), \frac{T_{2s}}{T_1} = \frac{T_3}{T_1} \left(1 - \frac{1}{rp^{\frac{k-1}{k}}}\right) - (rp^{\frac{k-1}{k}} - 1)v$$

Process (2-3): isobaric heat supply, $q_{2,3} = h_3 - h_2$, $w_{mech,2,3} = 0$. (4)

Process (3-4): isentropic expansion, $w_t = c_p(T_3 - T_{4s})$. (5)

State (4-1): isobaric heat release, $q_{4,1} = c_p \cdot (T_1 - T_{4s})$. (9)

There are differences between the ideal Brayton cycle and real gas turbine cycle. In the real cycle, the following are included:

1. Difference between the ambient air condition and the compressor inlet condition at point 1.
2. There are heat loss and friction losses in the compression and expansion processes, and thus these are not really isentropic processes.
3. Gas properties vary with temperature and not constants as assumed in the ideal cycle.
4. There is stagnation pressure loss in the combustion chamber and incomplete combustion.
5. Some of the air discharged from the compressor is extracted to the turbine for cooling.

The losses in compressors are usually expressed through the following:

1. By the compressor efficiency defined by

$$\eta_c = \text{ideal work of compression} / \text{actual work of compression}$$

2. By assuming the compression is adiabatic but with friction

2.2. The GT performance

The simple cycle in an $h-s$ diagram including losses is shown in Figure 6a.

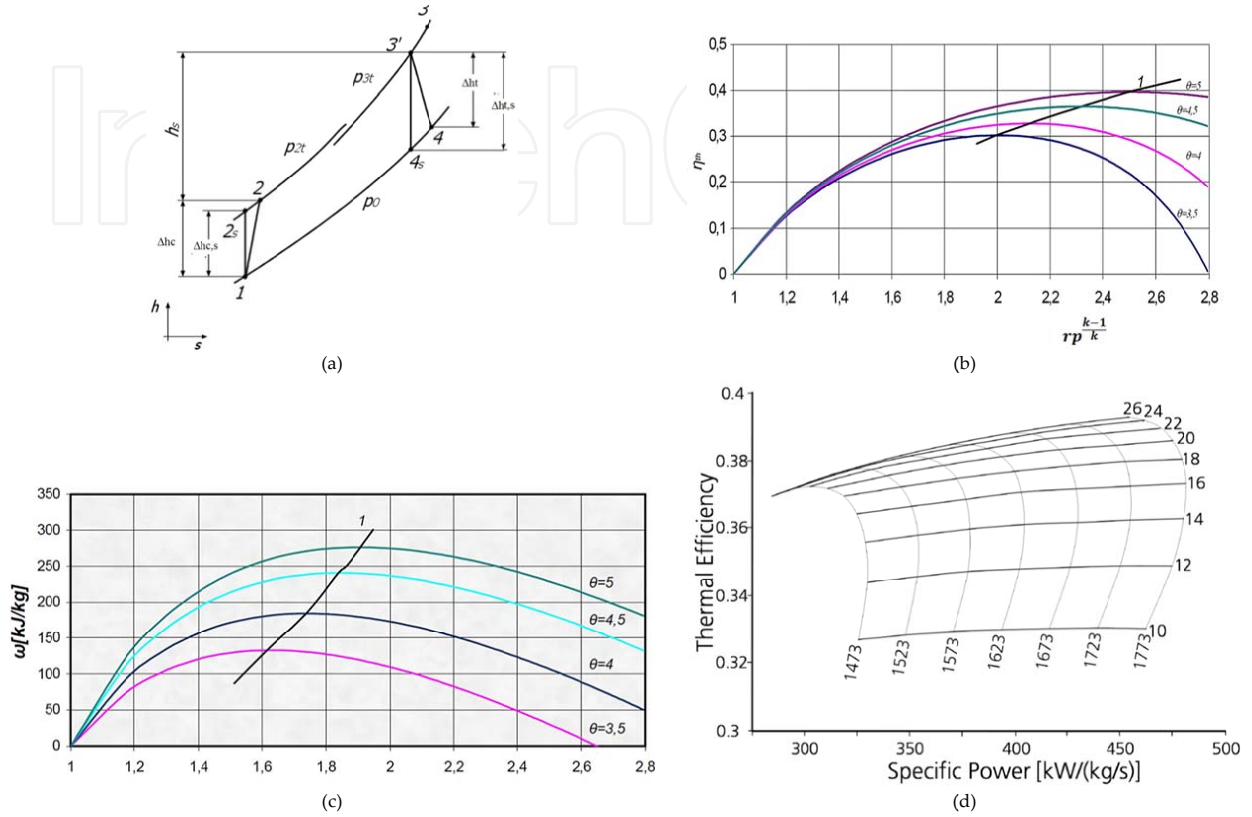


Figure 6. a: Enthalpy-entropy ($h-s$) diagram for ideal and practical gas turbine cycle [7] b: Dependence of the thermal efficiency η_{th} of the cycle on the parameters rp , k , and θ for $\eta_{t,is} = 0.88$ and $\eta_{c,is} = 0.86$. Line 1 joins points of maximum efficiency for each curve [7] c: Dependence of the specific work of the cycle on the parameters π , κ , and θ for $\eta_t = 0.88$ and $\eta_c = 0.86$. Line 1 joins points of maximum specific work for each curve [7] d: Thermal efficiency vs specific power for varying pressure ratios (10–26) and combustor outlet temperature (1,473–1,773 K) for a gas turbine [8]

$$\eta_c (\text{cycle efficiency}) = (h_3 - h_4) / (h_3 - h_2)$$

$$\eta_{t,is} (\text{turbine isentropic efficiency}) = (h_3 - h_4) / (h_3 - h_{4s})$$

$$\eta_c (\text{compressor isentropic efficiency}) = \frac{w_{c,is}}{w_c} = \frac{h_{2s} - h_1}{h_2 - h_1}$$

$$= \frac{\frac{k}{k-1} RT_1 \left[\left(\frac{P_2}{P_1} \right)^{\frac{k-1}{k}} - 1 \right]}{h_2 - h_1} = \frac{k}{k-1} RT_1 \left[\left(\frac{P_2}{P_1} \right)^{\frac{k-1}{k}} - 1 \right] / C_p (T_2 - T_1)$$

The losses in turbines are usually expressed by the turbine efficiency defined by

$\eta_t = \text{actual work of expansion} / \text{ideal work of expansion}.$

Assuming that θ is the ratio of the turbine inlet temperature and compressor inlet temperature, which in this case is $\theta = T_3/T_1$,

$$\eta_c = \frac{\frac{T_3}{T_1} \eta_{t, is} \left(1 - \frac{1}{rp^{\frac{k-1}{k}}} \right) - \frac{1}{\eta_{c, is}} (rp^{\frac{k-1}{k}} - 1)}{\left(\frac{T_3}{T_1} \right) - 1 - \frac{1}{\eta_{c, is}} (rp^{\frac{k-1}{k}} - 1)}$$

The efficiency of the thermodynamic cycle depends mainly on the TIT (T_3) or its dimensionless parameter $\theta = T_3/T_1$ as well as the pressure ratio rp as shown in Figures 6b–d. The highest cycle temperature is limited by the material and cooling of the first turbine stages; pressure ratio can be optimized to maximize the efficiency for a specific combustor temperature. Besides optimization of the efficiency, the gas turbine is also optimized for power output (Figure 6d). The optimization sets the conditions for the combustor. For the gas turbine cycle in Figure 6 at a combustor outlet temperature at 1,743 K, the optimal pressure ratio for specific power is 14:3 bar and the optimal pressure ratio for efficiency is 25:1 bar. These values are engine specific but show the tendency for optimization. The efficiency of the thermodynamic cycle depends mainly on the TIT (T_3) or its dimensionless parameter $\theta = T_3/T_1$ as well as the pressure ratio rp .

The thermal efficiency always increases with the increase of θ or the TIT, T_3 , which has limitation with the materials. The pressure ratio rp ($P_2/P_1 = P_3/P_4$) affects the cycle efficiency, which increases with rp until it reaches a maximum and then starts to fall. The optimal compression ratio changes with alteration of the compressor and turbine efficiencies.

The specific work, defined by the work per unit mass of the air, increases T_3 and reaches a maximum for a certain rp as shown in Figure 6c.

Two distinct losses occur in the combustion chamber: combustion inefficiency and pressure loss.

The first implies an imperfect conversion of the chemical energy in the fuel/air mixture into thermal energy. It is defined as

$$\eta_{cc} = \frac{\bar{c}_p \left[(\dot{m}_{air} + \dot{m}_f) T_{t3} - \dot{m}_{air} T_{t2} \right]}{\dot{m}_f \Delta h_u}$$

The typical combustion efficiency is around 0.99 or better.

The thermal efficiency of a real gas turbine cycle is lower than the one of the ideal cycle. In the T-s diagram or in the P-v diagram, respectively, the differences are obvious since there are no more isentropic changes possible.

2.3. Gas Turbine (GT) components

GTs are operating according to Brayton cycle and using the following components.

2.3.1. Air intake

The air to compressor should pass through an air filter to prevent dust from entering the machine and is accelerated in a duct to the compressor. The inlet duct in front of the compressor is usually designed as a diffuser. This decelerates the air at the inlet and converts part of the air kinetic energy into pressure.

Figure 7a shows an air filter installed at the air inlet to the compressor. The inlet air duct can contain an air cooling system. The compression in the GT is a constant volume process. So, the air temperature decrease would increase the air density and mass flow rate, decrease the specific power consumed by the compressor (per unit mass), and increase the GT power output. Figure 7b shows the effect of compressor inlet temperature on the GT output power and heat rate. The air inlet temperature can be decreased by evaporative cooling, fogging, and chilled water system as shown on the psychrometric chart given in Figure 7c.

Figure 8a shows an inlet air to compressor using evaporative cooling which used relative humidity and wet bulb temperature that are rather low. This system has the advantage of low capital and operation cost as it can operate on raw water and uses air washer that cleans the inlet air. Figures 8b–d show an inlet air to compressor using fogging system. It is also an evaporative cooling system that is used when relative humidity and wet bulb temperature are rather low. This system uses demineralized water and increases GT performance better than the previous evaporative cooling system.

Figure 9a shows mechanical refrigeration system (direct type) used hot in areas and can bring the air temperature to any specific requirement irrespective of ambient temperature and humidity ratio. This system has the advantage of increasing the GT performance better than evaporative cooling and fog system. However, this system has high initial capital cost and high operation and capital cost. Figure 9b shows the absorption refrigeration system (direct type), which is similar to that of Figure 9a, but with absorption cooling system operated mainly with steam or hot water substituting the mechanical refrigeration system. This systems has also the advantage of increasing the GT performance better than evaporative cooling and fog system, but at higher initial capital cost and high operation and capital cost.

2.3.2. GT compressor

The main parameters of a compressor are the required pressure ratio (r_p), volumetric flow rate, consumed power, and permissible shaft length. The used compressors types in GT application are axial, centrifugal, and combination of both. Axial compressors have more stages to reach the same compression ratio achieved by centrifugal type, and thus, axial compressors have a longer shaft than centrifugal ones. Axial compressors have lower changes of flow direction during compression and thus better efficiency (82–90 %) compared to centrifugal (72–82 %). Axial compressors handle much wider range of volume flows, are used

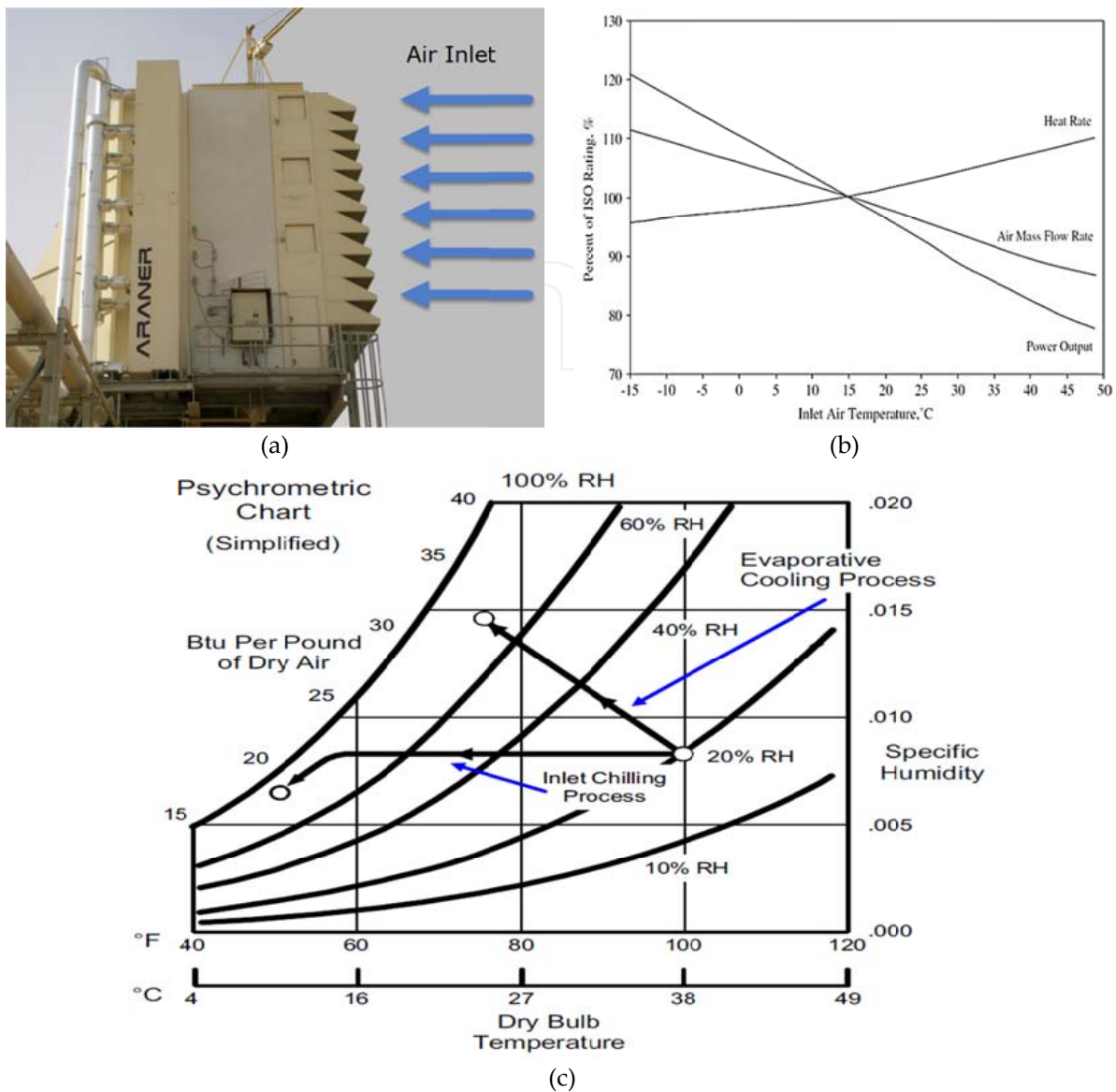


Figure 7. a: Turbine inlet air cooling filter-house modification to place the cooling coil coming from ammonia compression chiller plant [9] b: Typical inlet air cooling impacts on combustion turbine performance [1] c: Psychrometric chart showing evaporative cooling process and chilled water cooling process [10]

in all heavy utility gas turbines, have much lower tendency for flow separation at the inlet blades, and are more reliable in the case of fast load changes. Centrifugal compressors have small-size, short shafts, used only in small gas turbines (less than 5 MW) and high rotor speeds. Combination of axial and centrifugal compressors utilizes axial compressor reliability and the centrifugal compressor high-pressure ratio.

In centrifugal compressor (Figure 10a) the air (to be compressed) enters the impeller center and moves outward by centrifugal force to the compressor discharge diffuser. The rotating impellers accelerate the air velocity, and the air kinetic energy is converted to an increase in static pressure by slowing the flow through a diffuser before being discharged.

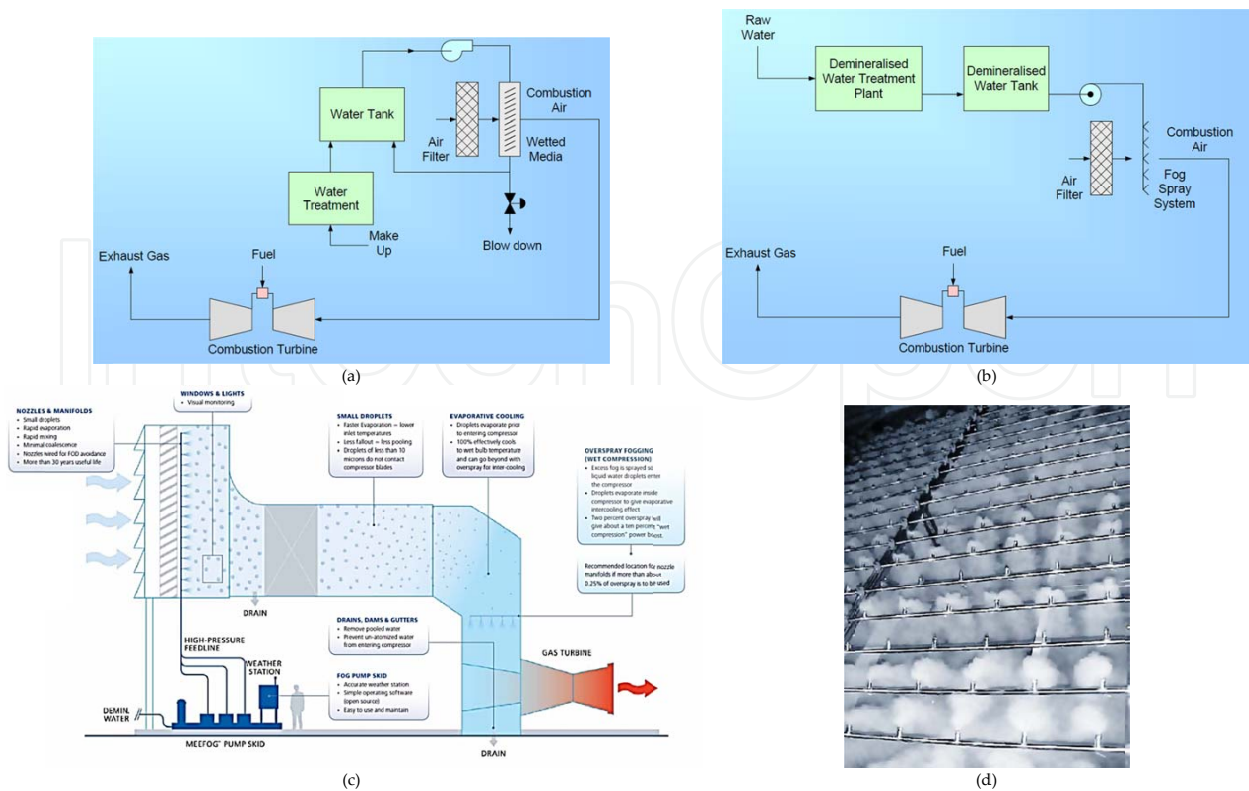


Figure 8. a: An inlet air to compressor using evaporative cooling which used relative humidity and wet bulb temperature that are rather low [11] b: An inlet air to compressor using fogging system which used relative humidity and wet bulb temperature that are rather low and using demineralized water [11] c: Fog system produces billions of microfine (10-micron average) droplets at 2,000 psi that create a much larger overall evaporative surface, which allows the droplets to evaporate and cool the airflow far more quickly than larger, heavier droplets. This results in faster, more effective evaporation and cooling with significantly lower drain water rates [12] d: MeeFog™ array for a frame 7FA gas turbine, Mee Industries – Fogging Systems for Offshore Gas Turbines

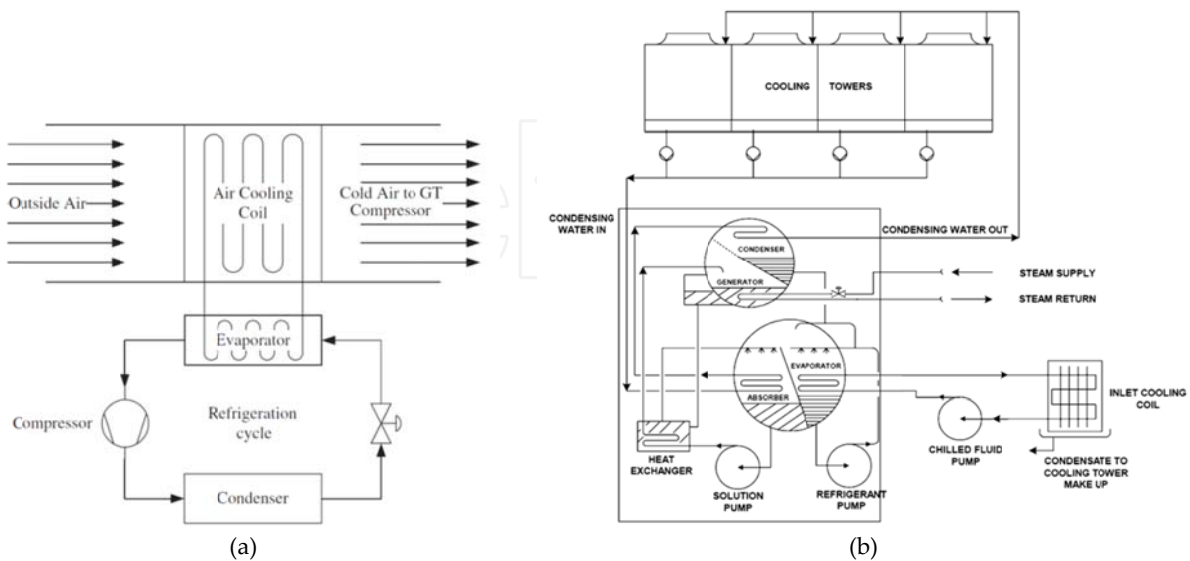


Figure 9. a: Mechanical refrigeration system (direct type) used in areas where relative humidity is rather high [1] b: Absorption refrigeration system (direct type) used in areas where relative humidity is rather high [1]

Axial compressors have moving (rotor) and fixed (stator) blades (Figure 8b). The arrays of blades are set in rows, usually as pairs: one rotating and one stationary. While rotating airfoils (known as blades or rotors) accelerate the fluid, the stationary airfoils (known as stators or vanes) decelerate the air, i.e., slow it down, and its kinetic energy is converted to pressure energy. The stators redirect the flow direction for the rotor blades of the next stage. The discharge velocity is almost equal to the suction velocity. This process is repeated by several stages depending on the desired output pressure.

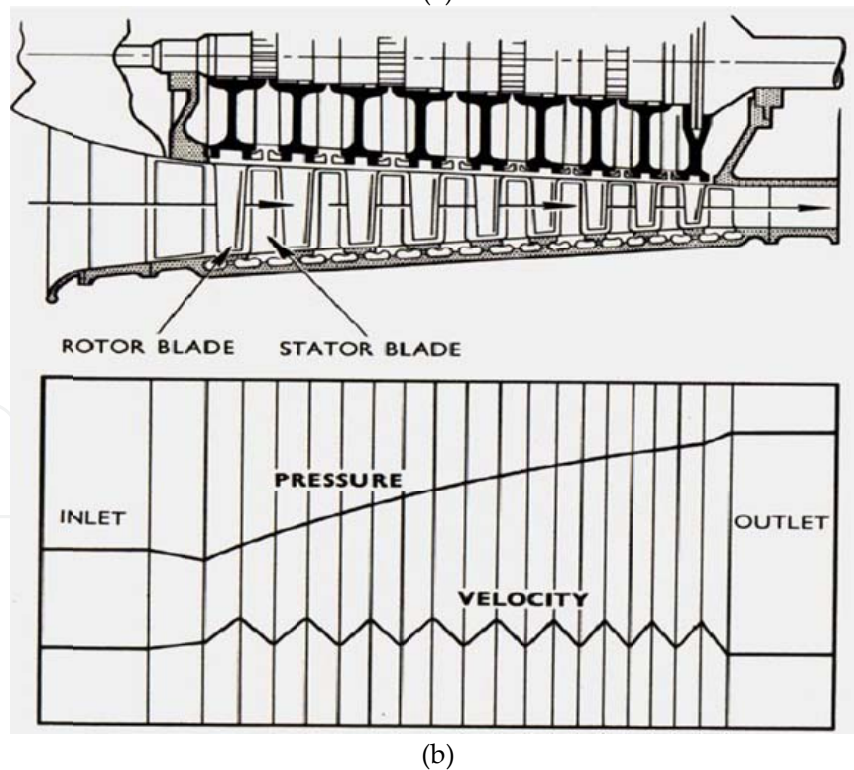
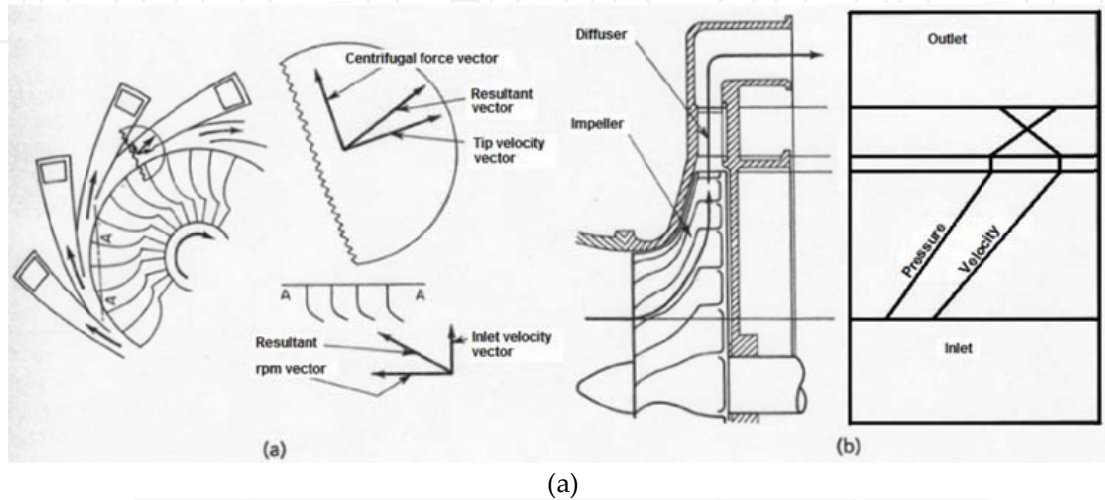


Figure 10. a: Centrifugal-compressor flow, pressure, and velocity changes; (a) airflow through a typical centrifugal compressor and (b) pressure and velocity changes through a centrifugal compressor [13] b: Schematic diagram of an axial flow compressor and pressure and velocity profile [14]

The direction of flow is parallel to the direction of the rotation. The design of compressor blades is different than those of turbines. The compressor blades have divergent profile and act as diffuser to increase air pressure. The turbine blades have convergent profile which works as a nozzle, reducing air pressure by changing its pressure energy into kinetic energy. More on axial compressor design is given in Ref. [15]. Although an axial stage may not offer as much of pressure ratio as a centrifugal stage of the same diameter, a multistage axial compressor offers far higher pressure ratio (and therefore mass flow rates and resultant power) than a centrifugal design.

Separation of the air flow from the surface of the blades of the first compressor stage is real problem in axial and centrifugal compressors. Flow separation from the surface of single blades generates high turbulence in the grid and can partly block the flow path of the incoming air aerodynamically. This effect, called a rotating stall, stresses the whole gas turbine structure with oscillating pressure waves.

2.3.3. GT combustor

The compressed air leaving the compressor is directed to the combustion chamber (cc), called combustor, where fuel such as natural gas (or petroleum liquids) is injected. In a combustor (Figure 11a) the fuel chemical energy is converted to thermal energy. So, the combustor combines and mixes air and fuel, ignites them, and contains the mixture during combustion. The combustor contains basically four zones – primary zone, secondary zone, dilution zone, and various wall jets – to manage heat transfer at the combustor boundary as shown in Figure 11b. Air entering the combustor is distributed to four major injection points. The first is through swirl vanes positioned at the combustor front face and typically surround the fuel injection port. The swirl vanes impart a circumferential velocity component to the air and thereby thrust the air radially outward as the air enters the combustor (Figure 11c). This creates a pressure void at the center line and induces a backflow to fill the centerline pressure deficit. This effectively creates, as a result, a recirculation flow that extends approximately one duct diameter downstream and defines the “primary zone” of the combustor.

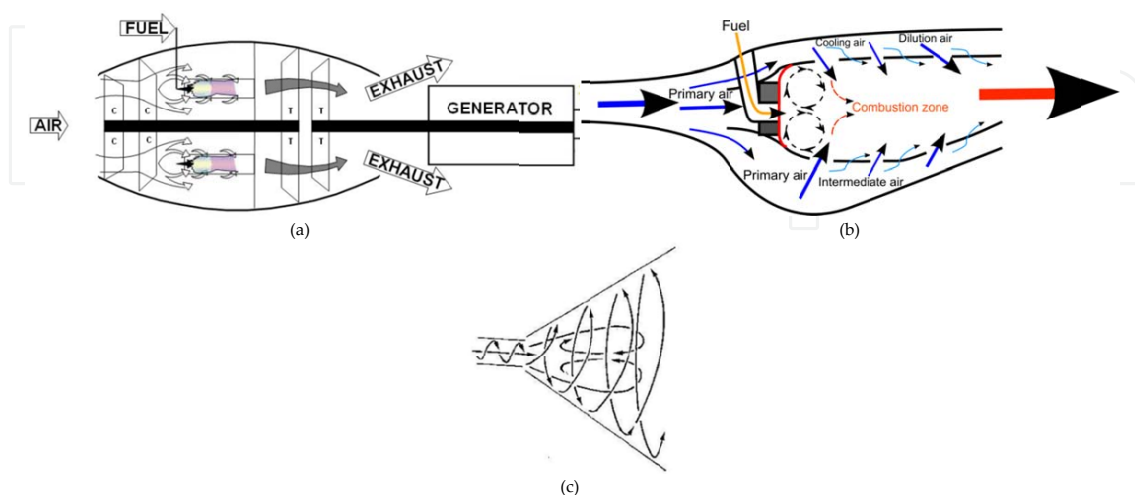


Figure 11. a: Stationary gas turbine electric power generator [16] Figure 11b: Schematic illustration of a general combustor [8] c: Circulation created by air swirler

The combustors are classified as:

1. Annular (continuous chamber that encircles the air in a plane perpendicular to the air flow) (Figure 12a)
2. Can-annular (similar to the annular but incorporates several can-shaped combustion chambers rather than a single continuous chamber) (Figures 12b, c)
3. Silo (silo, frame-type, combustor has one combustion chamber mounted externally to the gas turbine body)

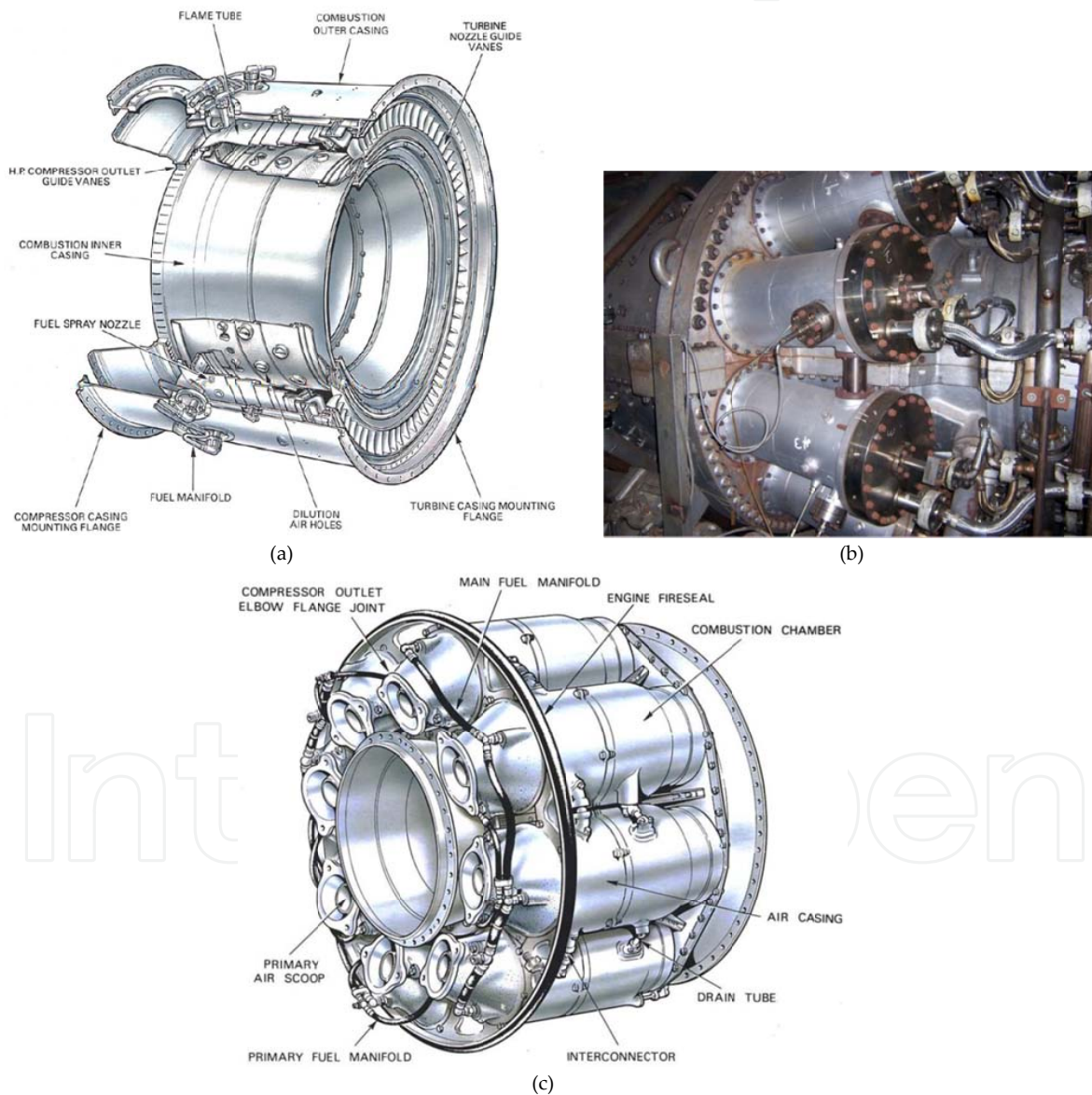


Figure 12. a: Annular combustion chambers [17] b: Gas turbine combustor arrangement [5] c: Several combustors arranged equidistant on the same pitched circle diameter, and each consists of an inner flame tube or liner cylinder mounted on the same axis inside an outer casing cylinder, called tubular combustors [18]

The combustion process in the GT combustor can be classified as diffusion flame combustion or lean-premix staged combustion. In the diffusion flame combustion, the fuel/air mixing and combustion take place simultaneously in the primary combustion zone, and this generates regions of near-stoichiometric fuel/air mixtures where temperatures and NO_x generation are very high. In lean-premix combustion, fuel and air are thoroughly mixed in an initial stage resulting in a uniform, lean, unburned fuel/air mixture which is delivered to a secondary stage where the combustion reaction occurs [19]. The combustion process starts with mixing the fuel with air supported by natural or forced turbulences in the airflow through the combustor. Continuous and stabilized combustion process is affected by the speed of fuel and air particles to the reaction zone, transport of flue gas from there, the speed of the chemical reaction in the reaction zone, and the residence time of any particle in the reaction zone. When the air-fuel mixing is slow compared to the chemical reaction rates, the mixing time controls the burning rate.

In diffusion flames, fuel and oxygen are mixed in the reaction zone through molecular and turbulent diffusion and have wide stability rate of combustion process. It has the advantages of relatively simple design of the fuel nozzles. Since the local conditions at the flame front are rich in fuel, diffusion combustion is insensitive against combustion instabilities and keeps on burning and generates regions of near-stoichiometric fuel-air mixtures with very high temperatures even at very lean conditions. The high temperature by diffusion flames leads to the production of large quantities of thermal NO_x .

To reduce the reaction temperatures and/or the formation of thermal NO_x , premix combustion is developed, where fuel and air are homogeneously mixed in an initial stage to become lean, unburned fuel-air mixture which is delivered to a secondary stage where the combustion reaction takes place. Manufacturers use different types of fuel-air staging, including fuel staging, air staging, or both; however, the same staged, lean-premix principle is applied. Gas turbines using staged combustion are also referred to as Dry Low NO_x combustors. The majority of GT currently manufactured are lean-premix staged combustion turbines.

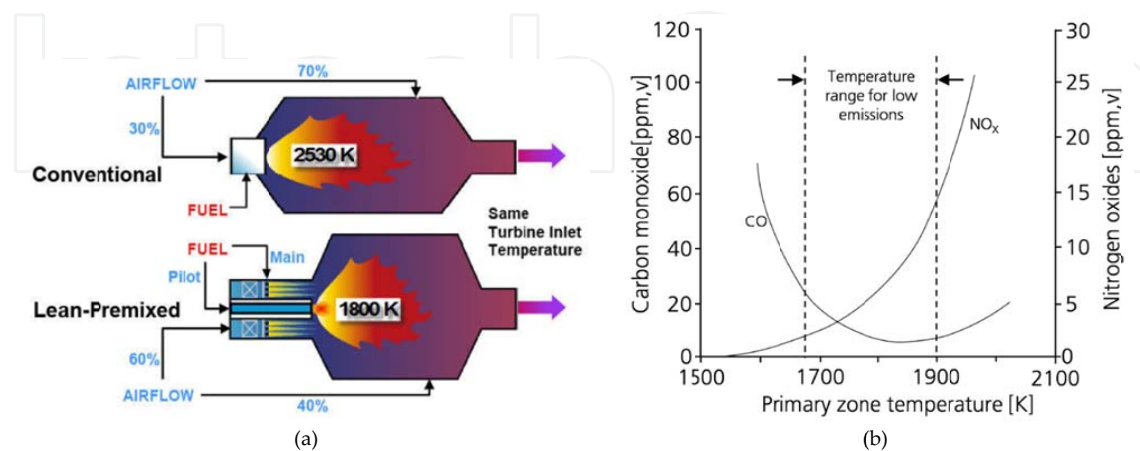


Figure 13. a: Schematic of a conventional and a lean-premix combustor [20] b: Primary zone temperature influence on NO_x and CO emissions [8]

In premix, mixing of fuel and air occurs far before the reaction zone. Depending on the burner design and the flow velocity, the time from the fuel injection to the moment of ignition is within several milliseconds. This time is used to create a mostly homogeneous mixture, with a fuel concentration within the ignition range of the specific fuel for the given compressor discharge temperature. The typical adiabatic flame temperature, to which a premix combustion system is adjusted, is at 1,750 K. At this temperature, the formation of NO_x is still on an acceptable level, while the heat transfer from the flame is high enough to ensure the ignition of the fresh mixture (Figures 13a, b).

In general, there is an operation window for low emissions that range from the primary zone temperatures 1,670 K to 1,900 K (Figure 13b). The upper temperature limit is set by the temperature dependence of NO_x and the lower limit by carbon monoxide. The increase in CO for lower temperatures is related to poor combustion and the lean blowout limit for the burner.

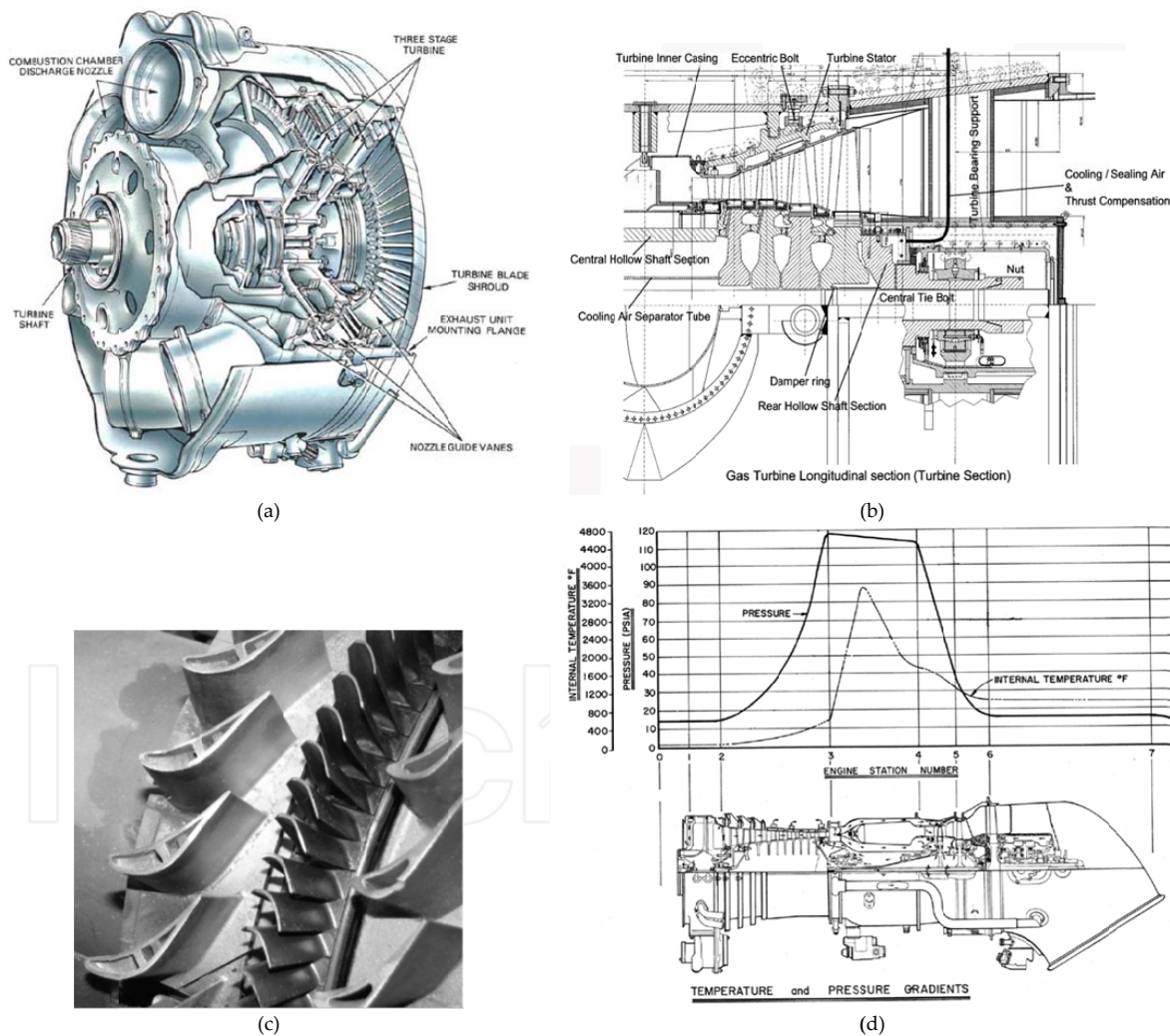


Figure 14. a: A triple-stage turbine with single-shaft system [17] b: The gas turbine section of the Siemens V94.2 gas turbine. c: Turbine stage with stators to the left which have the main function to act as nozzles to increase the velocity of the gas primarily in the tangential direction, by converting pressure energy to kinetic energy. To the right of the stators are the rotors, which have the function to convert the kinetic energy to power by causing a rotation of the shaft [4] d: Temperature and pressure throughout gas turbine [18]

2.3.4. GT turbine

The hot gases produced in the combustor are expanded in the turbine (Figures 14a–d) to give mechanical energy that operates the compressor, and the balance produces the electric power (EP). The turbine, similar to the compressor, can be axial or centrifugal type. The axial type is easier to cool, as the turbine is exposed to high thermal stresses by the hot gases entering the turbine. The turbine cooling is crucial as it provides the potential of raising the TIT and thus the efficiency. Gas turbines can be particularly efficient when heat content of the hot gases from the turbine is recovered in HRSG to power a conventional ST in GTCC. The hot gases from the GT can also be used for space or water heating or drive an absorption chiller for cooling the inlet air and increase the power output. Figure 14d shows that the hot gases leaving the GT are high enough to generate steam.

3. The Combined Gas-Steam Turbine Cycle (GTCC)

3.1. The GTCC overview

The exhaust gases leaving the GT can have high temperature (up to 600 °C) and use a heat recovery steam generator (HRSG) to generate steam. This steam can operate thermally driven desalting units such as multistage flash (MSF) (Figures 15a, b)) or multi-effect thermal vapor compression (ME-TVC) desalting systems or can operate steam turbine (ST). Combination of GT, HRSG, and ST cycle forms GTCC (Figure 15c) of much higher efficiency than single-cycle PP using GT or ST. A schematic diagram of steam turbine (Rankine) cycle components that can be combined with GT is shown in Figure 16a. Large steam turbine is usually divided into high-pressure (HP), intermediate-pressure (IP), and low-pressure (LP) cylinders (Figure 16b). In GTCC, the GT cycle is called the upper cycle, the steam turbine is called the bottom cycle, and both cycles are shown on T-s diagram in Figure 17a. Modern ST power generation, as shown in Figure 16a, is based on the Rankine cycle which includes the ideal basic cycle processes of (a) isentropic expansion in the steam turbine (ST) from 3-4 and from 5-6; (b) condensation of the steam discharged from the ST in the condenser from 6-1; (c) reversible adiabatic pumping process of condensate from condensing to the HRSG pressures, 1-2; and (d) heat addition at constant pressure in the steam generator (SG) to raise feedwater to saturation temperature, evaporate it, and superheat it from 2-3. In reheat steam cycle, the steam leaving the HP section returns to the SG from 4-5 for further heating before being admitted to the IP cylinder. Reheat is sometimes necessary to raise the steam dryness fraction at the turbine exit than the minimum of 0.88 required by the industry to avoid the blades pitting and raise the efficiency of the LP cylinder.

The use of GTCC to produce both EP gives high-energy utilization factor (UF), up to 80 %, where

$$UF = (\text{Work output} + \text{process heat})/\text{fuel heat supplied}$$

The GTCC is usually used for baseload operations because of its high efficiency. The HRSG can have single-, double-, or triple-pressure stages. The HRSG of single and double-pressure stages and their temperature distribution are shown in Figure 17b. A bottoming steam cycle using double-pressure steam HRSG is shown in Figure 18a. A triple-pressure stage HRSG is shown in Figure 18b. Several differences exist between the steam PP cycle using conventional steam generator (SG) (Figure 19a) and steam cycle in the GTCC (Figure 19b) using HRSG of the GT. The ST plant in Figure 19a has 300 MW electric power (EP) output capacity, using reheat cycle where steam leaving the HP cylinder is reheated in the SG before its introduction to the IP cylinder. This cycle has five closed feed heaters and one open feed heater (deaerator), and the steam flow rate leaving the condenser is 197.86 kg/s, about 76 % that of throttling condition (261.1 kg/s).

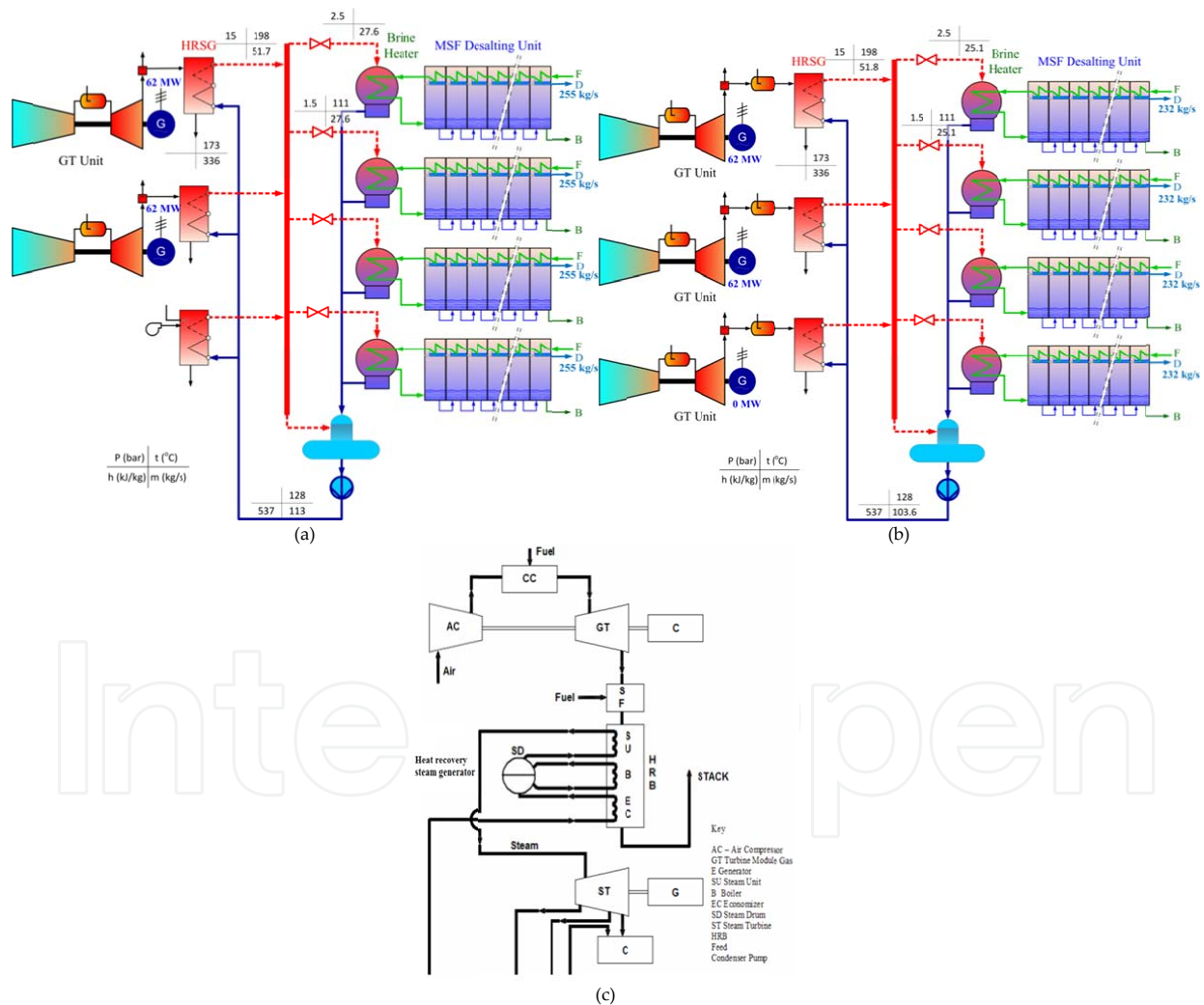


Figure 15. a: Two GTs conned to two HRSGs generating steam to operate two MSFs and using standby boiler [21] b: Three GTs conned to two HRSGs generating steam to operate three MSFs and using auxiliary burners to operate the HRSG [21] c: GTCC with GT, HRSG, and steam turbine (ST)

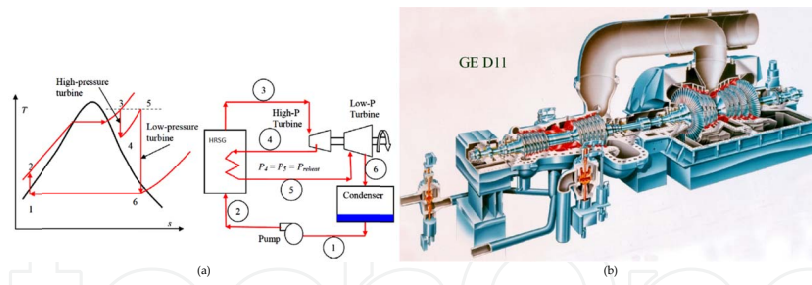


Figure 16. a: Schematic steam turbine (Rankine) using high-pressure (HP), intermediate-pressure (IP), and low-pressure (LP) cylinders b: Steam turbine with HP, IP, and LP cylinders

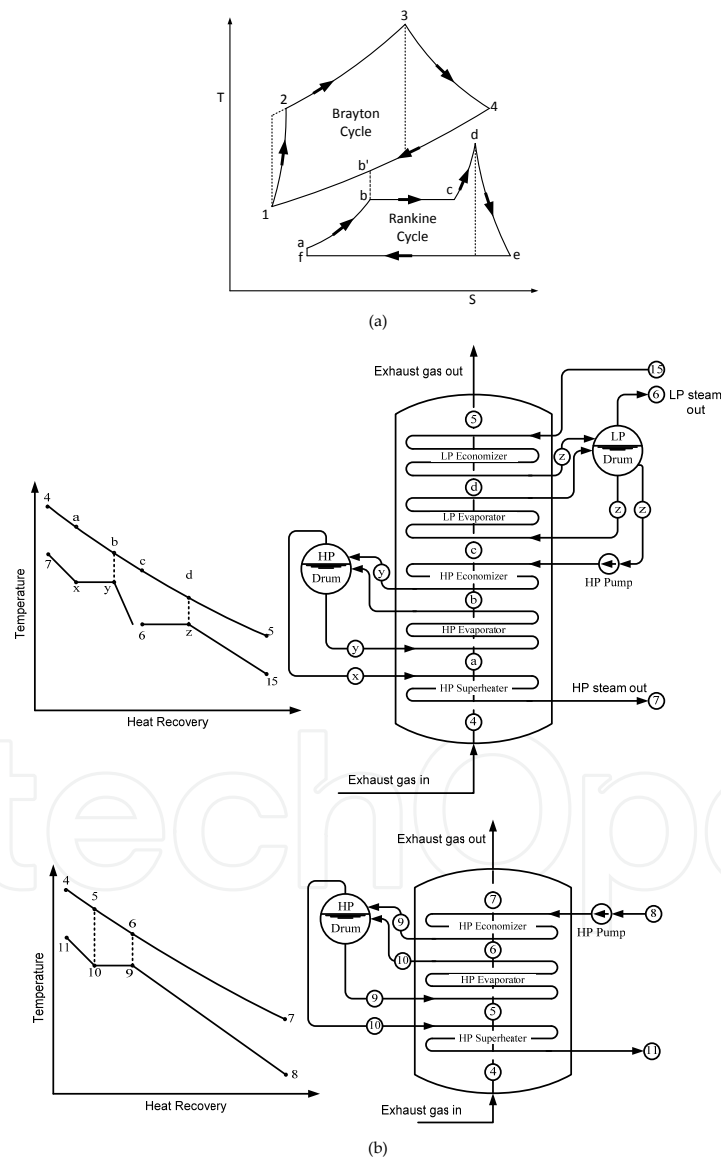


Figure 17. a: Upper GT turbine cycle (Brayton) and bottom Rankine steam cycle. b: HRSG of dual pressure in the middle and single pressure at the bottom steam stages and their temperature distribution [20]

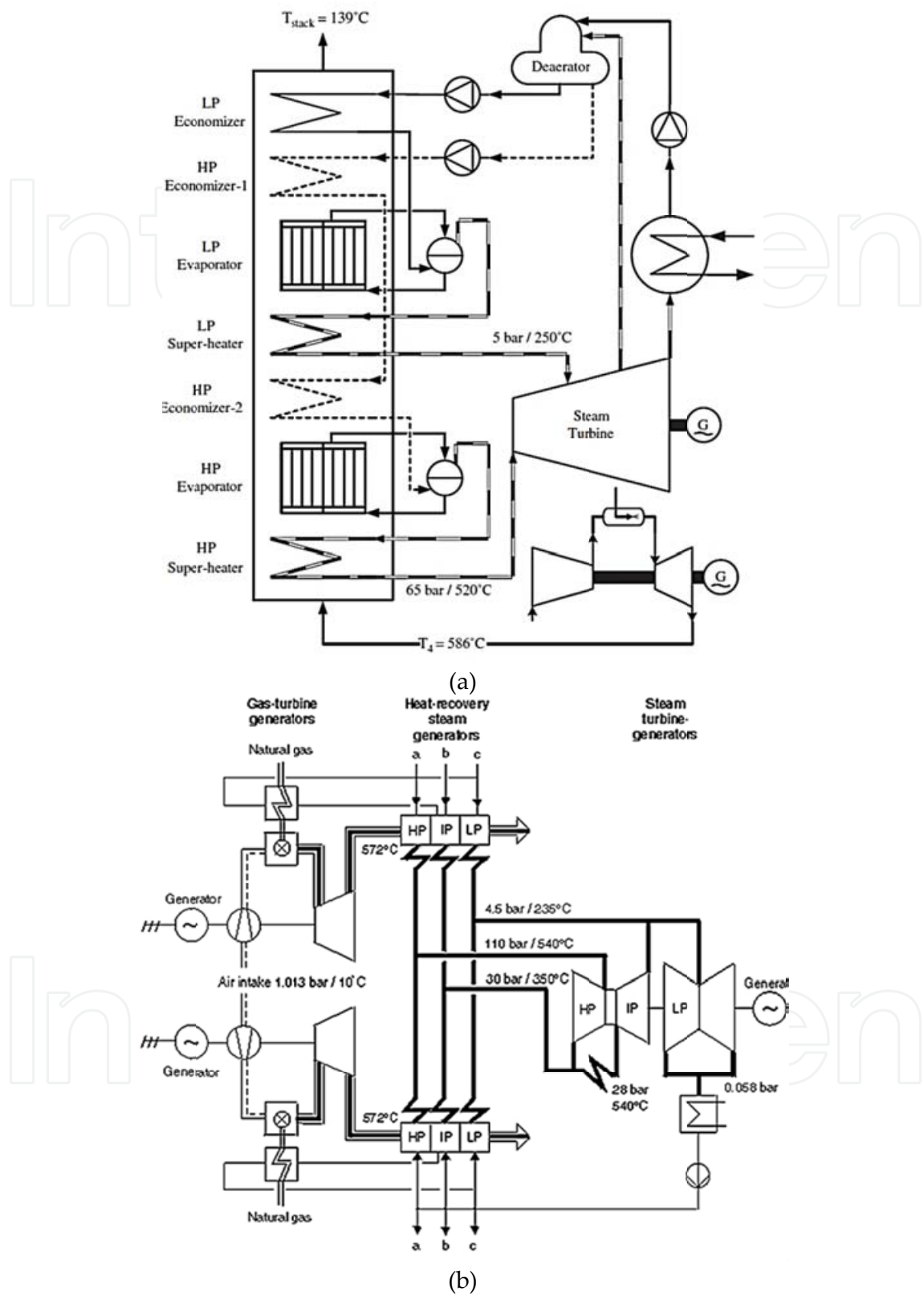


Figure 18. a: Bottom steam cycle with dual-pressure steam stages HRSG [1] b: GTCC using triple-pressure steam HRSG [23]

The ST cycle shown in Figure 19b and with data given in Table 3 is also a reheat cycle of 275 MW output capacity. It utilizes the hot gases leaving three GTs of 164 MW of EP output each. Contrary to the cycle in Figure 19a, the cycle using the HRSG has no feed heaters as all feedwater heating is done in the HRSG, and thus, the steam flow rate leaving the condenser is 438.8 kg/s, about 123.3 % that of throttling condition (355.3 kg/s), and the steam to the ST is admitted from the three stages HRSG to the ST at three points (pressures); see Figures 19a,b .

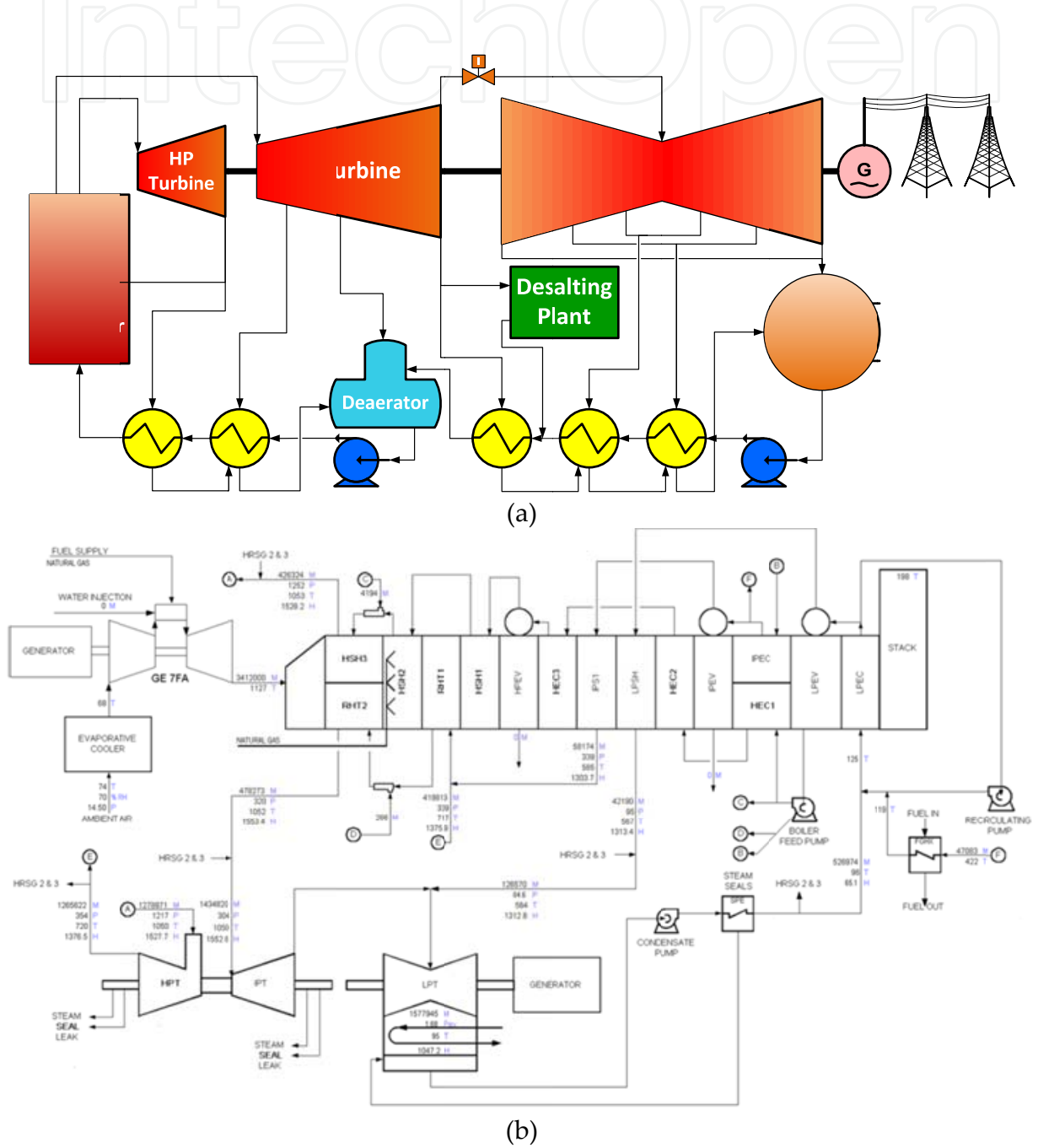


Figure 19. a: Conventional steam power plant operated by fuel-operated steam generator. b: Combined GTCC using 3 GT, 3 HRSG, and one steam turbine [5]

Case	Case 1: 74 °F ambient temperature, unfired
Ambient temperature, °F, relative humidity 70 %	
GT capacity	3×164.1 MW
GT fuel	NG
Total GT output	492.3 MW
Steam turbine output	275.55 MW
Total gross EP output	767.850
Auxiliary power	18.45 MW
Net EP output	794.4 MW
Gross GT heat rate, BTU/kWh (LHV), Btu/kWh	9,310
Gross GT fuel consumption (LHV)	4,583.3
NPHR, Btu/kWh, (LHV)	6,116
Net plant efficiency, % (LHV)	44.8

Table 3. Data of the GTCC given in Figure 19b [5]

3.2. Steam turbines in GTCC

The steam turbine in the GTCC can be extraction-condensing steam turbine (ECST) (Figure 20a) or back pressure steam turbine (BPST) (Figure 20b). In the ECST, steam is expanded from inlet pressure (say at 100 bar) and high temperature (up to 538 °C) to the condenser pressure (about 10 kPa) below atmospheric pressure. As steam expands, its pressure and temperature decrease, while its specific volume and its volumetric flow rate increase. This requires increasing the blade length of the turbine as steam expands to accommodate the increased volumetric steam flow (Figure 20c). In large-scale steam turbines, the steam volumetric flow is limited by the size of the turbine last stages (see Figure 16b), and this can enforce the use of double-flow condensing steam turbine where the last stage flow is divided between two rows of blades.

In BPST, the steam exits the turbine at the pressure required by the process to be heated as desalination, say 2–3 bar and is higher than that in the end condenser of the ECST cycle, say at 10 kPa. Condensation of discharged steam in industrial processes provides process heat needed for desalination, heating, absorption cooling, or any other processes.

The steam expansion in the ST is usually represented on the enthalpy-entropy (called Mollier chart) as turbine line shown in Figure 21a. For an adiabatic process, the change in enthalpy Δh is equal to the specific work, w per kg of flowing steam. The steam line on the h - s diagram would be a vertical line in reversible (ideal) expansion. The entropy increases during expansion in actual adiabatic process on a Mollier chart. The end point of the irreversible process still lies on that constant-pressure line corresponding to the exhaust pressure. Figure 21a shows that an increase in entropy during expansion decreases the work output, since the change $\Delta h(\text{actual})$

is less than $\Delta h(isentropic)$ as the isentropic efficiency defined by: $\eta(isentropic) = \Delta h(actual) / \Delta h(isentropic) < 1$.

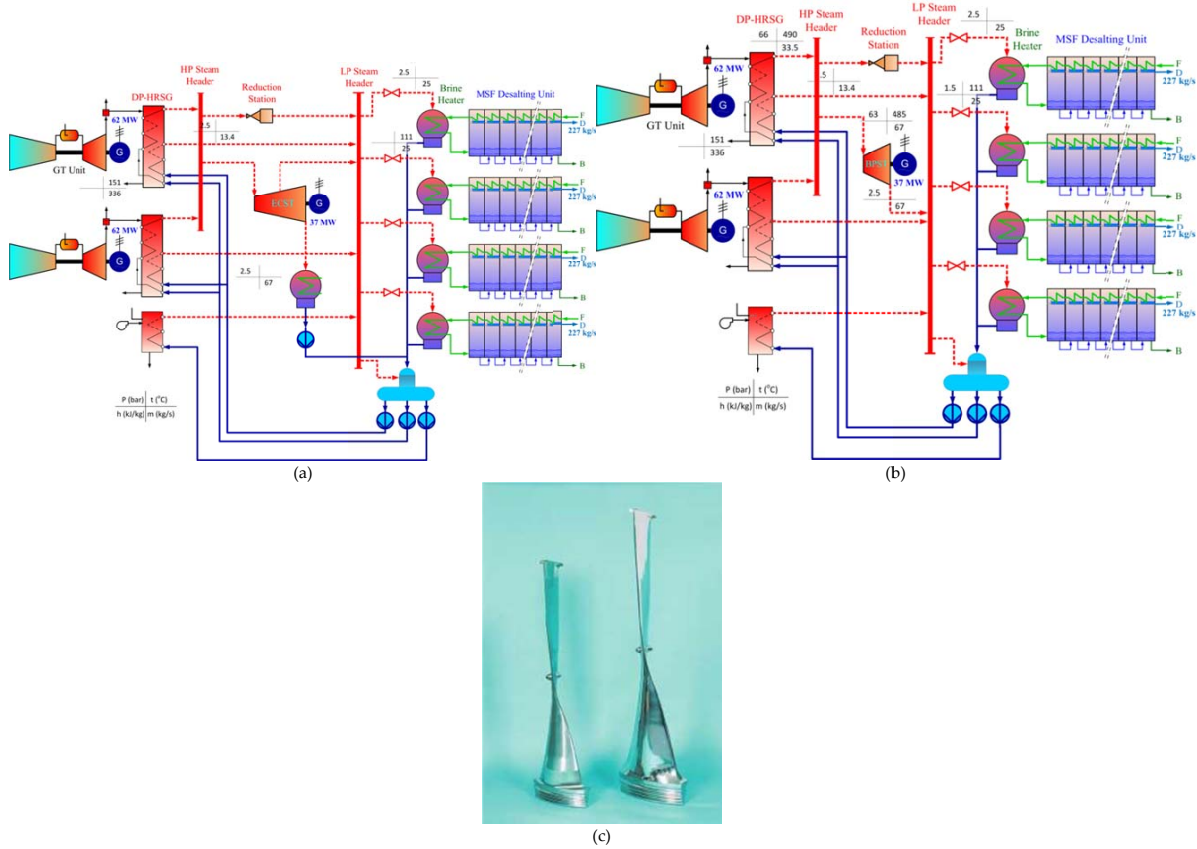


Figure 20. a: GTCC with GT, HRSG, and using extraction condensing steam turbine (ECST) [21] b: GTCC with GT, HRSG, and using back pressure steam turbine (BPST) and standby boiler [21] c: The new last stage buckets come in two sizes – 85 cm and 1.21 m [24]

One of the main concerns in the design of the ST is its exhaust size selection discharging to the condenser. Lowering the condenser pressure allows more expansion of the steam in the ST, i.e., more decrease in the enthalpy Δh that is transferred to work. However, decreasing the pressure increases the steam specific volume, thus increasing the steam velocity and increasing the kinetic energy loss of the steam as it leaves the turbine to condenser at almost zero velocity. Figure 21a shows that for the turbine line ABC on the h-s diagram, the exit steam dryness fraction is about 0.84, which is less than 0.88 and not acceptable. Once reheating is done, line ED, the dryness fraction increases to 0.92, which is acceptable. Figure 21b illustrates the exhaust loss curve for a condensing steam turbine. The exhaust area for a particular application should provide a balance between exhaust loss and capital investment in turbine equipment.

Some of the GTCC mount the GT and ST on the same shaft (Figures 22a, b). Since the steam turbine comes to operation after heating up the whole steam cycle, a freewheel clutch is installed between the steam turbine and the generator to prevent the GT from spinning up the steam turbine in a cold steam cycle. Due to the freewheel clutch, the shafts of the gas turbine

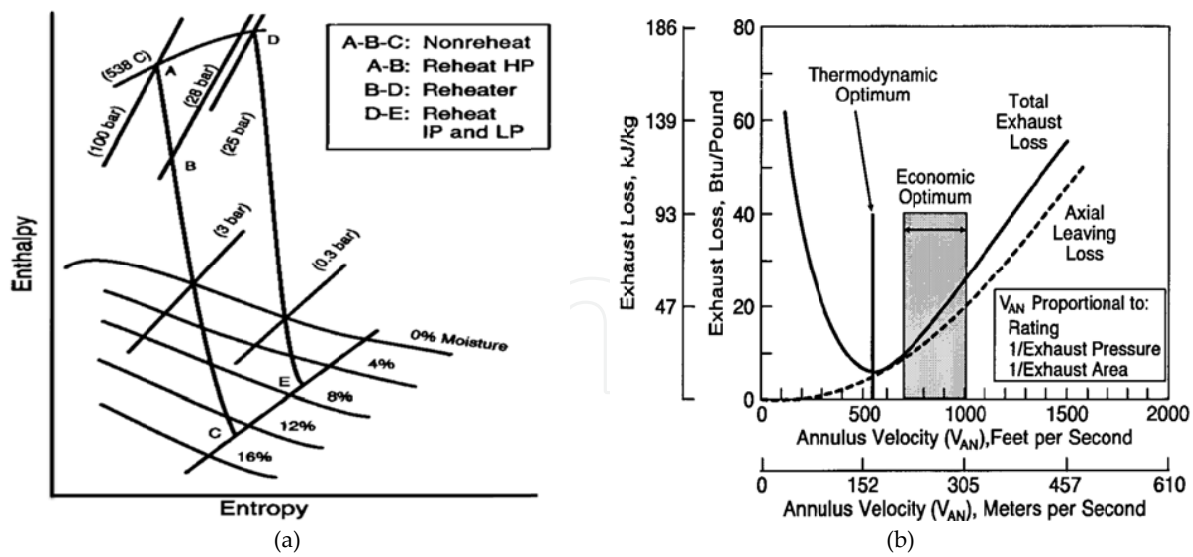


Figure 21. a: Enthalpy-entropy diagram for a steam turbine [25] b: Illustrative exhaust loss curve [25]

and the steam turbine are spinning up separately, which prevents them from reaching speed ranges that would cause dangerous resonance frequencies. As soon as the boiler is heated up to operation temperature, the control valve is opened and the steam turbine provides its part of power to drive the generator [23].

Figure 22a shows the ST mounted on the same shaft of the GT and both use the same generator, one GT and one ST of single- and double-flow LP cylinders as developed by GE. In addition, the steam turbine can be combined with single GT but with separate shafts or several gas turbines and one ST and several shafts as shown in Figures 22a, b.

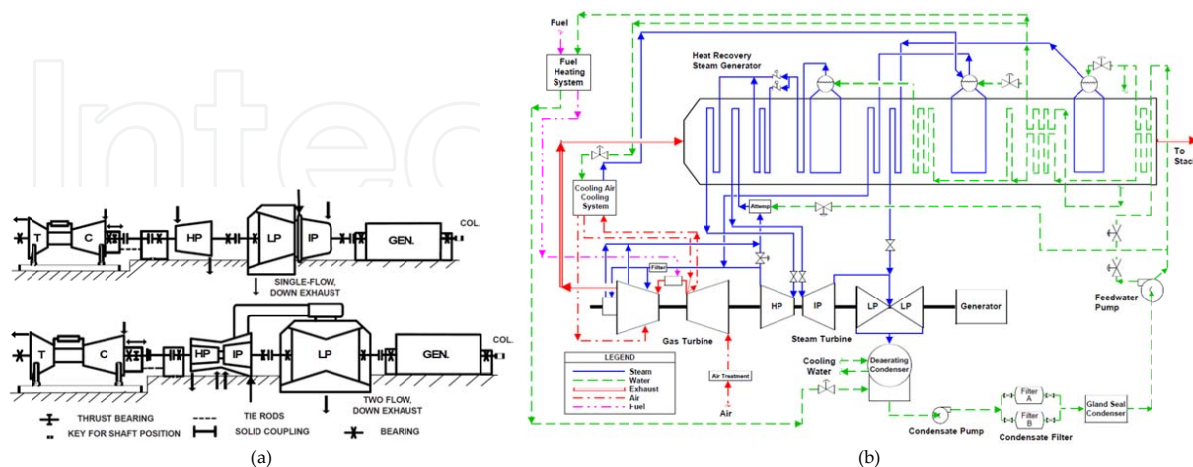


Figure 22. a: S107H and S109H single-shaft steam turbine and GT (STAG) equipment configuration [26] b: STAG 107H/109H cycle diagram [26]

3.3. Cogeneration steam turbine

Steam can be extracted from ST for processing heat by using a nonautomatic extraction ST that has openings in the turbine casing for steam extraction, with no means for controlling the pressure of the extracted steam. Steam can also be extracted from an automatic extraction steam turbine with openings in the turbine casing for extraction and means for directly regulating the steam flow to the next turbine stages after extraction opening. Automatic extraction turbines are used when there is a need for process steam at specific pressure between turbine inlet and outlet pressures, as in the case of desalination. There is simultaneous control of the desired extraction steam pressure and turbine speed, even though the demand for extraction steam and the power requirements of the driven load may vary over a wide range. Also an induction-extraction ST that can admit and exhaust steam. In extraction condensing steam turbine (ECST), the steam or part of it exits the turbine at a given pressure and may further be used. The 300 MW steam turbine operating in Kuwait provides full steam demand to two MSF desalting units of 7.2 MIGD each when the turbine EP load varies between 300 and 75 MW.

In Kuwait CPDP, the MSF unit gain ratio defined by desalted water (DW) output to heating supply S (i.e., D/S) has a typical value of 8, and the steam pressure at extraction point to the MSF at full load is 3.5 bar and is throttled to the pressure required by the MSF of 2 bar. When the turbine load is lowered, the steam pressure throughout the turbine is also lowered and reaches about 2 bar at the MSF extraction point when the turbine load is 25 % of the 300 MW nominal load. So, a throttling valve between the extraction point and the MSF is installed to keep the pressure to the MSF plant at 2 bar (Figure 19a). If the steam at the extraction point is less than 2 bar, extraction to the MSF is stopped. In this case, if the MSF can work directly from the high pressure steam supply to the turbine after being throttled and desuperheated (Figures 23a, b).

Steam condensation in the DP provides the steam latent heat as the heating source to the DP. The specific work produced by expanding steam from throttling condition of P_1 and T_1 to the condenser pressure P_o and T_o is represented by the area encircled by ABCDA in Figure 24a and the area BEFC, represents the specific rejected heat. When steam is extracted at P_3 to the DP, the specific work per kg of steam is represented by AGHD in Figure 23b, and the area GBCH is the work loss for each kg extracted to the DP. In the Kuwaiti plant, the steam to the MSF unit is extracted from crossover pipe between the intermediate-pressure (IP) and the LP cylinders (Figure 23b). So, the ratio of power to water outputs in CPDP varies as the EP load is always variable and cannot be stored, while water depends on the demand and available storage capacity. So, the EP and DW production ratio is not always constant or matched together.

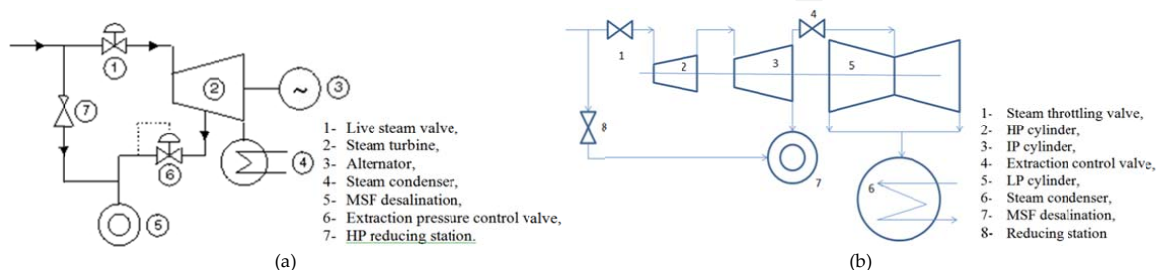


Figure 23. a: Case 1. HP-LP cylinder features for steam extraction from turbine casing [28] b: Case 2. HP-LP cylinder features for steam extraction from crossover pipe between IP and LP cylinders [28]

Steam condensation in the DP provides the steam latent heat as the heating source to the DP. The specific work produced by expanding steam from throttling condition of P_1 and T_1 to the condenser pressure P_0 and T_0 is represented by the area encircled by ABCDA in Figure 24a and the area BEFC, the rejected heat. When steam is extracted at P_3 as in Figure 24b to the DP, the specific work per kg of steam is represented by AGHD in Figure 24b, and the area GBCH is the work loss for each kg extracted to the DP.

It is noticed here that in BPST, the steam flow to the turbine depends on the turbine load, and thus, the steam discharged to the DP is slave to the turbine load. So, BPST is usually used in baseload operation, and steam to the DP can be supplied from HP steam line, which is very expensive.

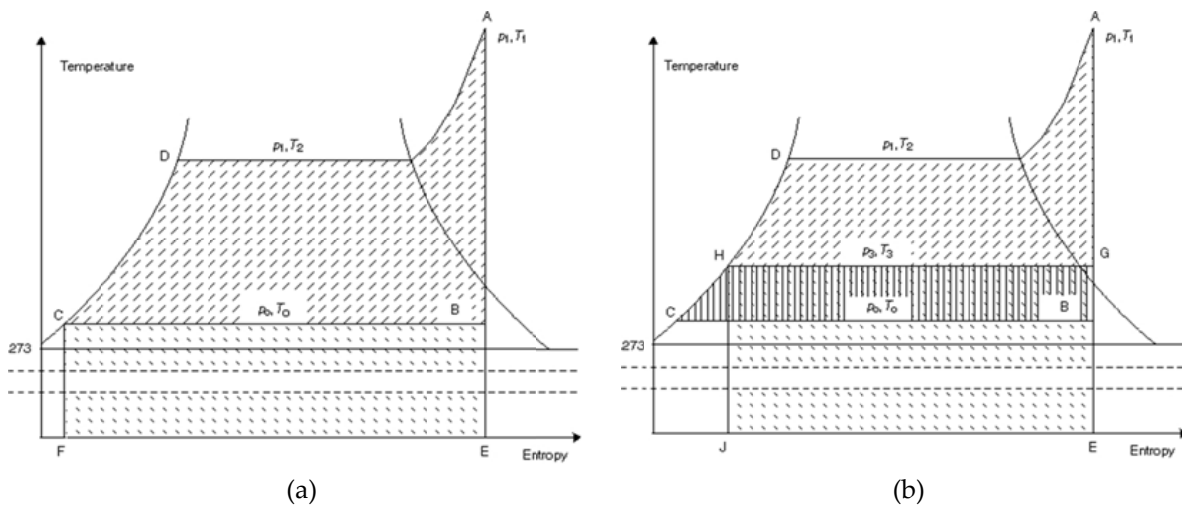


Figure 24. Enthalpy-entropy diagram for a steam cycle of (a) power-only plant and (b) dual-purpose plant [23]

3.4. Heat Recovery System Generator (HRSG)

The HRSGs utilize the hot gases leaving the GT to generate steam that can be used to operate thermally driven desalting plants or steam turbines bottoming power cycle. The HRSG can be unfired, supplementary fired or called post-fired (PF), and fully fired. The HRSG can be horizontal or vertical (Figures 25a–d). As given before, the HRSG can have single-, dual-, or triple-pressure level type. The single-pressure stage HRSG has low efficiency, compared to dual-pressure HRSG. In single-pressure HRSG, high efficiency is attained by lowering the stack temperature, and this requires lowering the steam pressure. Lowering the steam pressure lowers the steam cycle efficiency. In dual-pressure designs, lowering stack temperatures would only decrease the first (low)-stage pressure while leaving the second state conditions approximately unchanged. A design parameter of the HRSG is the pinch point (pp), which is the temperature difference between the gas leaving the boiling section and generated steam saturation (or boiling) temperature. The choice of high pp increases the mean temperature difference between the hot gases and water and reduces the heat transfer area but decreases to a certain extent the HRSG efficiency. The low-pressure (LP) generated steam in dual-

pressure HRSG can feed the steam turbine at a suitable point or it may be used as process steam for industrial applications (drying, desalination, absorption refrigeration, etc.).

In CPDP, electricity and process heat for desalination are simultaneously produced regardless of gas turbine load; supplementary firing or post-firing (PF) is usually used. In Ras Laffan B CPDP, a very flexible plant design was developed with PF to allow very high thermal power input (maximum 280 MWth) to cope with a wide operational range of GT electrical power and steam production for electricity or desalinated water production. The power island having a total capacity of 1025 MW is equipped with three V943A gas turbines with bypass stack to allow open-cycle operation, three HRSGs equipped with double PF firing, and two 200 MW range backpressure steam turbines; steam from the power island is fed to four desalination units supplied by Doosan for a total water production of 273,000 m³ per day. Each GT has 310 MW power output at generator terminals, 39.8 % efficiency, and 750 kg/s exhaust gas mass flow rate at 576 °C exhaust gas temperature.

The HRSGs are of the horizontal gas flow, top supported, natural circulation type, with single-pressure stages, and two-staged supplementary firing. The HRSG steam parameters at full GT load are pressure = 85.4 bar and temperature = 563 °C, 636 t/h nominal, and 703 maximum steam flow.

The post-firing modified the steam flow as follows: first firing increased the steam flow to nominal 110 t/h and maximum 145 t/h, and second firing increased the steam flow rate to nominal 150 t/h and 170 t/h.

4. Cost allocation in CPDP utilizing GTCC

This section develops a mathematical model to evaluate the performance of a typical CPDP using typical GTCC plant and how this performance is affected by parameters such as ambient temperature, compression ratio, air-to-fuel ratio, turbine inlet temperature, and stack temperature. The fuel consumed by the GT is allocated to each of the products (EP and DW) on the basis of the first and second laws of thermodynamics [30].

Figure 26 shows a schematic diagram of a typical CPDP using GTCC, which is considered as reference plant considered here. The plant's design is based on the data given in Table 4 and 50 °C ambient summer temperature and 600 °C temperature of exhaust gases leaving the GT.

No. of units	Fuel type	LHV	Gross output	Ambient temp.	Humidity	Pressure
3	NG	47,806 kJ/kg	215.5 MW	50 °C	30 %	1.013 bar
HRSG, type: natural circulation			Desalination: MSF	Steam turbine, ST: BPST		
No. of HRSG	Integral type deaerator	HRSG blowdown	No. of units and capacity	No. of ST	Gross capacity, MW	Cooling SW temperature °C
3	3	1 %	3×15 MIGD	1	215.7 MW	°C

No. of units	Fuel type	LHV	Gross output	Ambient temp.	Humidity	Pressure
GTCC						
Gross GTCC output, MW			Net GTCC output, MW			
862.2 MW			819.7 MW			

Table 4. Technical specifications of Shuaiba North GTCC power-desalination plant Gas turbines GE912FA

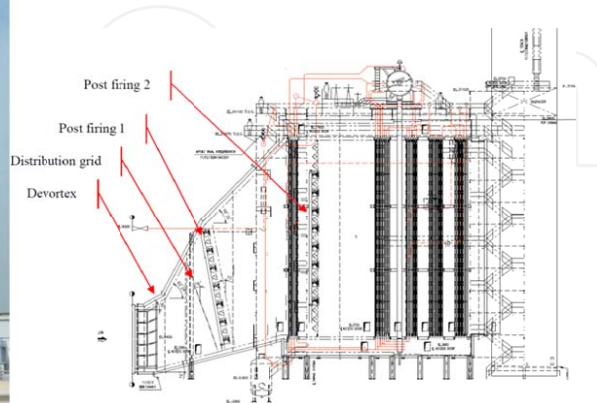
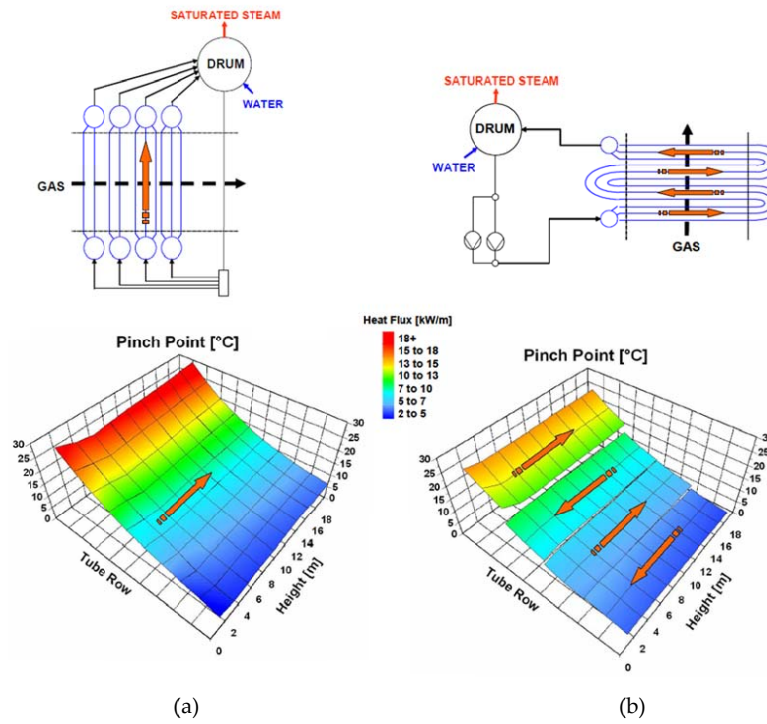


Figure 25. (a) Vertical and (b) horizontal, HRSG LPEVA arrangement and pinch diagram Figure 25c: Ras Laffan B HRSGs [29] Figure 25d: Ras Laffan longitudinal section, single pressure [29]

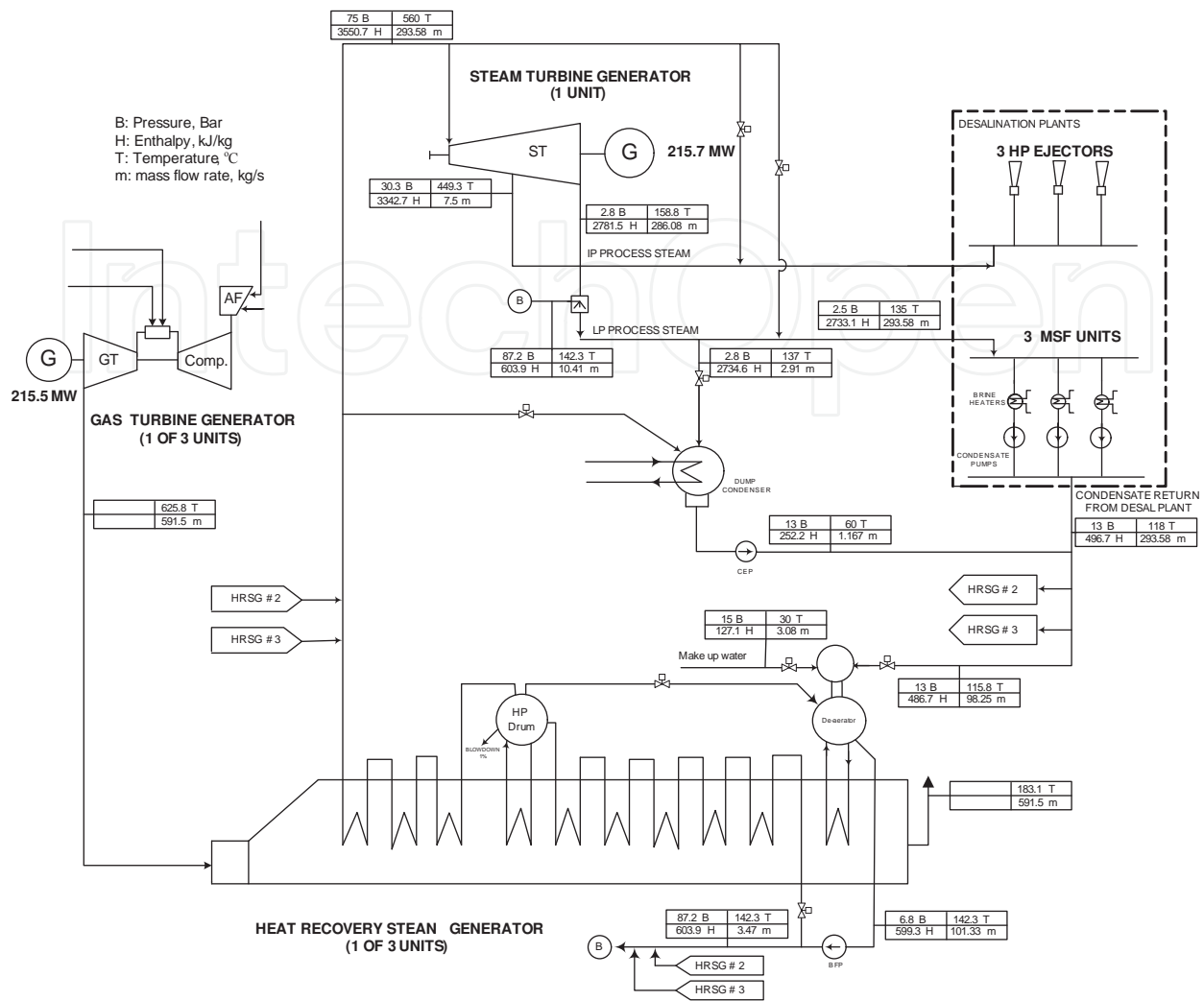


Figure 26. Mass and heat balance diagram of Shuaiba North GTCC power-desalination plant

4.1. Energy analysis

An energy analysis, based on the first law of thermodynamics, is given as follows.

4.1.1. Gas Turbine (GT) cycle

The GT cycle data give 625 °C exhaust gases exit temperature, 50 °C ambient temperature, and 215.5 MW power output for each GT. The isentropic efficiency is 0.85 for the compressor and 0.9 for the turbine. The mechanical efficiency is 0.998 for the turbine and 0.995 for the compressor.

The used fuel is NG having 47.806 MJ/kg low heating value (LHV) and 12.897 kg/s (45 t/h) flow rate. The airflow rate to each GT is 578.62 kg/s. The air-to-fuel ratio (A/F) is then 44.86; and the exhaust gases flow rate from each GT is 591.52 kg/s.

The compressor work is

$$W_c = m_a \times \frac{(h_2 - h_1)}{\eta_{mc}} = 578.62 \times \frac{(759.1 - 323.6)}{0.995} = 253.2 \text{ MW}$$

$$Q_f = m_f \times LHV = 12.897 \times 47,806 = 616.55 \text{ MW}$$

The heat gain by the air in is the combustion chamber

$$Q_{in} = m_a \times (h_3 - h_2) = 578.62 \times (1724 - 759.1) = 558.31 \text{ MW}$$

The turbine work output is

$$W_t = m_g \times (h_3 - h_4) \eta_m = 591.52 \times (1724 - 930.8) \times 0.998 = 468.25 \text{ MW}$$

The GT power output is

$$W_{GT} = (W_t - W_c) = 468.25 - 253.2 = 215.05 \text{ MW}$$

The gross GT cycle efficiency based on LHV is

$$\eta_{GT} = \frac{W_{GT}}{Q_f} = \frac{215.05}{616.55} = 0.35$$

4.1.2. Heat Recovery Steam Generator (HRSG)

There are three GTs, three HRSGs, and only one ST. One third (1/3) of feedwater from the steam cycle returns to each HRSG, and the heat gained by this feedwater is equal to that lost by the exhaust gases, then,

$$m_g \times C_p \times (T_4 - T_{stack}) = m_s \times (h_s - h_f)$$

where T_4 is the exhausted gas temperatures at the GT exit; T_{stack} is the HRSG stack exit; C_p is the gases' specific heat ($\sim 1.11 \text{ kJ/kg}^\circ\text{C}$); h_s and h_f are the specific enthalpies in kJ/kg of superheated steam leaving the HRSG and feedwater entering the HRSG, respectively; and m_s is the steam flow rate from each HRSG. The temperature profile of the hot gases and steam-water temperature in the HRSG is shown in Figure 27.

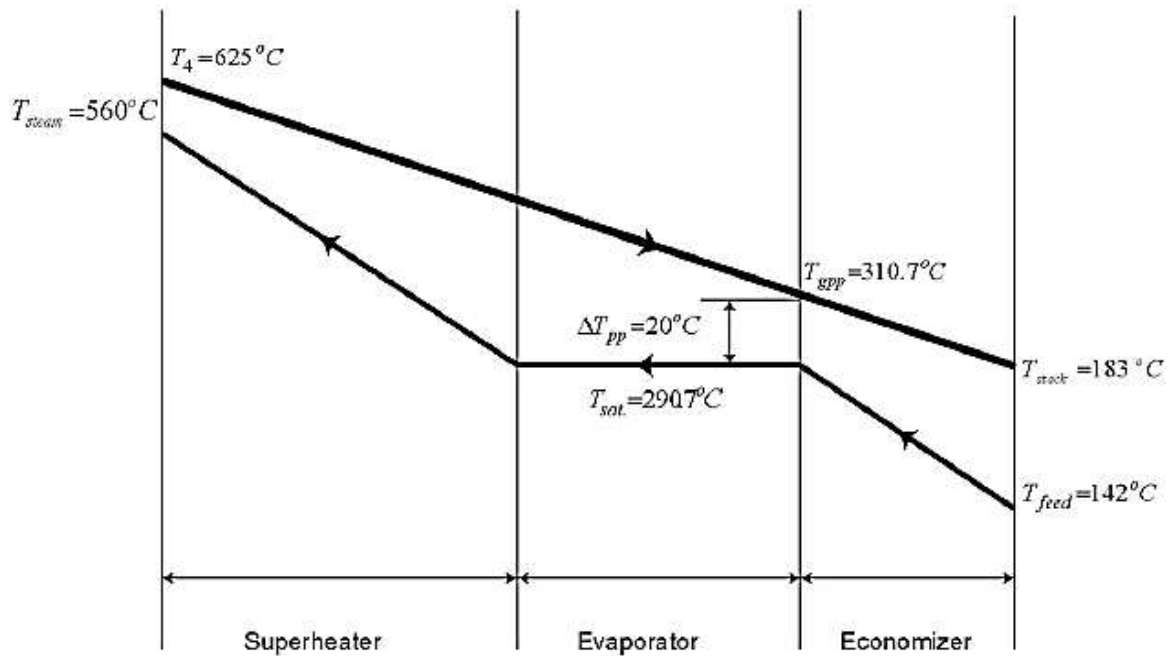


Figure 27. Gas and steam-water temperature profile of the HRSG

The superheated steam temperature T_s at the HRSG exit is determined by the terminal temperature difference ($T_4 - T_s$) with typical value in the range of 50 °C. The pinch point temperature (pp) difference is defined by the minimum temperature difference between the hot gases T_p and the steam saturation temperature, $pp = (T_p - T_{sat})$, say equal to 20 °C.

For the reference plant, $m_g = 591.5 \text{ kg/s}$, $T_4 = 625.8 \text{ °C}$, and $T_{stack} = 183 \text{ °C}$, and thus the heat loss from the hot gases is

$$m_g \times C_p \times (T_4 - T_{stack}) = 591.5 \times 1.11 \times \frac{625 - 183}{1000} = 290.7 \text{ MW}$$

The feedwater is heated from its inlet feed temperature to saturation liquid temperature T_{sat} , evaporated to saturated steam, and then superheated to T_s .

The steam leaving the three HRSGs is directed to the ST at mass flow rate, $3m_s = 1056.9 \text{ t/h}$ (293.58 kg/s) or $m_s = 97.86 \text{ kg/s}$ from each HRSG. The heat gain in the

HRSG by water, Q_{HRSG} is

$$Q_{HRSG} = m_s \times (h_s - h_f) = 97.86 \times \frac{3550.7 - 599.3}{1000} = 288.82 \text{ MW}$$

$3m_s = 1056.9 \text{ t/h}$ (293.58 kg/s) or $m_s = 97.86 \text{ kg/s}$ from each HRSG. The heat gain in the

HRSG by water, is Q_{HRSG}

This is almost equal the heat loss by hot gases; and the heat input to the steam cycle, Q_s , in from the three HRSGs is

$$Q_{s,in} = 3Q_{HRSG} = 3 \times 288.82 = 866,46 \text{ MW}$$

4.1.3. Steam cycle

The steam leaving the three HRSGs is directed to a back-pressure steam turbine (BPST). The steam discharged from the BPST enters the brine heaters of three MSF units.

The throttling condition of the steam inlet to the turbine is 75 bar pressure, 560 °C temperature, and 3,550.7 kJ/kg specific enthalpy. A small part of the expanded steam is extracted from the BPST to operate the steam ejectors of the MSF, at 30.3 bar, 449.3 °C, and 3,342.7 kJ/kg enthalpy, whereas the balance continues to expand and is exhausted to the three MSF units at 2.8 bar, 158.8 °C, and 2,781.5 kJ/kg enthalpy. This steam is desuperheated before entering the MSF units to 2.5 bar, 135 °C, and 2,733.1 kJ/kg enthalpy. The power generated by the BPST is

$$W_{st} = \left[\sum m_{in} h_{in} - \sum m_{out} h_{out} \right] \times \eta_{mech}$$

$$= (293.58 \times 3350.7 - 7.5 \times 3342.7 - 286.07 \times 2781) \times 0.99 / 1000 = 219.4 \text{ MW}$$

The power consumed by the steam cycle pumps in the steam cycle is negligible except that of the boiler feedwater pump (BFP), which can be calculated as follows:

$$W_{BFP} = \frac{v_f \times (P_{BFP} - P_{6.8})}{\eta_{BFP}} = 0.001408 \times (82200 - 680) / (0.8 \times 1000) = 4.3 \text{ MW}$$

The net power generated by the steam turbine is 215.1 MW, and the heat gained by the water in the three HRSGs is 866.46 MW. This gives the ST efficiency as

$$\eta_{st} = \frac{(W_{ST} - W_{BFP})}{Q_{in}} = \frac{(219.4 - 4.3)}{866,46} = 0.248$$

This efficiency underestimates the performance of the ST cycle. It does not account for the benefit gained by the steam leaving the ST to the MSF to produce desalted seawater and not expanded to an end condenser.

4.1.4. Desalination units

The heating steam mass flow rate to each MSF unit is $m_s = 97.86$ kg/s (one third of the steam discharged from the ST plus water used for its desuperheating). Each MSF unit produces desalted seawater (DW) at the rate $D = 15$ MIGD (789 kg/s). This gives gain ratio ($GR=D/S$) equal to mass of DW/heating steam = $789/97.75 = 8.06$

The heat consumed by each MSF unit is

$$Q_{de} = m_s \times (h_{d,in} - h_{d,ex}) = 97.86 \times \frac{2733.1 - 496.7}{1000} = 277 \text{ MW}$$

where $h_{d,in}$ and $h_{d,ex}$ are the enthalpy of steam entering the MSF brine heater and its return condensate, respectively.

So, the heat consumed for each 1 m^3 of desalted water is $q_d = (218.86 \times 1000) / 789 = 277 \text{ MJ/m}^3$.

It is more rational to express the heat supplied to the MSF by its real value in terms of mechanical equivalent energy. The turbine work loss due to discharging its steam to brine heater of MSF unit and not expanding to an end condenser can be calculated; if this steam was expanded in low-pressure (LP) turbine to condenser pressure at 10 kPa and dryness fraction of 0.9, its enthalpy would be 2,345.5 kJ/kg, and the produced work is

$$W_{de} = m_s \times (h_{MSF} - h_{cond}) = 97.86 \times \frac{2781 - 2345.5}{1000} = 42.7 \text{ MW}$$

This 42.6 MW is equivalent mechanical work W_{de} to the heat $Q_{de} = 218.86$ MW supplied to each MSF unit.

Another small amount of steam is extracted from the steam turbine at higher pressure to operate the steam ejectors of each MSF plant at 2.5 kg/s flow rate, 30.3 bar pressure, 449.3 °C temperature, and 3,342.5 kJ/kg enthalpy. If this steam was expanded in a turbine to the condensing pressure of 10 kPa and 90 % dryness fraction, its enthalpy would be 2,345.5 kJ/kg, and its work output is

$$Q_{ejector} = m_{ejector} \times (h_{ejector} - h_{cond}) = 2.5 \times \frac{3342.5 - 2345.5}{1000} = 2.4925 \text{ MW}$$

So, the work loss by the steam supplied to one 15 MIGD (789 kg/s) is

$$W_{th} = W_{de} + W_{ejector} = 42.6 + 2.5 = 45.1 \text{ MW},$$

and specific work loss is equal to

$$45,100 \text{ kW}/780 \text{ (kg/s)} = 57.16 \text{ kJ/kg} = 15.9 \text{ kWh/m}^3.$$

Since the pumping energy of the MSF is in the range of 4 kWh/m³ (14.4 kJ/kg), the total equivalent mechanical energy (counting for pumping and thermal energy) to produce 1 m³ of desalted water is

$$W_{\text{eq}} = W_{\text{th}} + W_{\text{pumping}} = 15.9 + 4 \cong 20 \text{ kWh/m}^3 = 72 \text{ kJ/kg}$$

So, the equivalent mechanical energy required to produce DW at the rate of 45 MIGD (2,367 kg/s) can be calculated as follows:

$$W_{\text{eq}} = 72 \times 2367 / 1000 = 170.424 \text{ MW}$$

This 170.424 MW consists of 34.1 MW for pumping energy and 136.34 MW for thermal energy.

The pumping energy of the BFP as well as for the MSF should be subtracted from the total power output of the turbines to become

$$\begin{aligned} \text{Net power output} &= 3 W_{\text{GT}} + W_{\text{ST}} - W_{\text{pump}} - W_{\text{BFP}} \\ &= (3 \times 215.02) + 215.1 - 34.085 - 4.3 = 821.77 \text{ MW} \end{aligned}$$

4.1.5. Total cycle

The fuel energy consumed by the three GT units is

$$Q_{f,t} = 3 \times Q_f = 3 \times 616.5 = 1849.5 \text{ MW}$$

The total power output from the GTCC is $3 W_{\text{GT}} + W_{\text{ST}} = 645 + 215.1 = 960.1 \text{ MW}$ and the GTCC overall efficiency $\eta_t = 960.1/1849.5 = 0.465$.

Again, this efficiency underestimates the performance of the GTCC, since it does not account for the heat gained by the 3 MSF units.

Another term is usually considered and known as the utilization factor (UF):

$$UF = \frac{3 W_{\text{GT}} + W_{\text{ST}} + Q_{de}}{Q_{f,t}} = \frac{645 + 215.1 + 218.86}{1849.5} = 0.82$$

where $Q_{f,t}$ is the only heat added to the three GT cycles.

In fact, the UF overestimates the performance of the CPDP since it adds the work by both GTs and ST (high-quality energy) to heat supplied to the MSF units $3 Q_{de}$ (low-quality energy).

A new modified total efficiency η_{mf} is

$$\eta_{mf} = \frac{3W_{GT} + W_{ST} - W_{pump} + W_{de}}{Q_{f,t}} = \frac{(645 + 215.1 - 34.1 + 170.43)}{1849.5} = 0.54$$

So, an energy balance of the given CPDP using GTCC and MSF units shows that $Q_{f,t}$ is supplied to the overall system, which is mainly converted partially to the following main items:

- a. Total work output by $3 W_{GT} + W_{ST} - W_{pump} - W_{BFP} = 3 \times 215 + 215.1 - 34.1 - 4.3 = 821.7$ MW (44.4 % net efficiency).
- b. Heat added to 3 MSF units, $Q_{des,t} = 3 \times Q_{de} = 3 \times 218.86 = 656.58$ MW (35.51 % of total heat input).
- c. The heat rejected to the environment in the form of hot gases leaving the three stacks of the HRSGs is

$$Q_{stacks} = 3 \times m_g \times C_p \times (T_{stack4} - T_e) = 591.5 \times 1.11 \times \frac{183.1 - 50}{1000} = 262.2 \text{ MW}$$

where T_e is the ambient temperature.

The balance will be unaccounted energy losses,

$$Q_{losses} = Q_f - 3W_{GT} - W_{ST} - 3Q_{de} - W_{stack} = 1849.4 - 645 - 215.1 - 656.58 - 262.2 = 70.52 \text{ MW}$$

Figure 28 shows the energy balance of the given GTCC and MSF units.

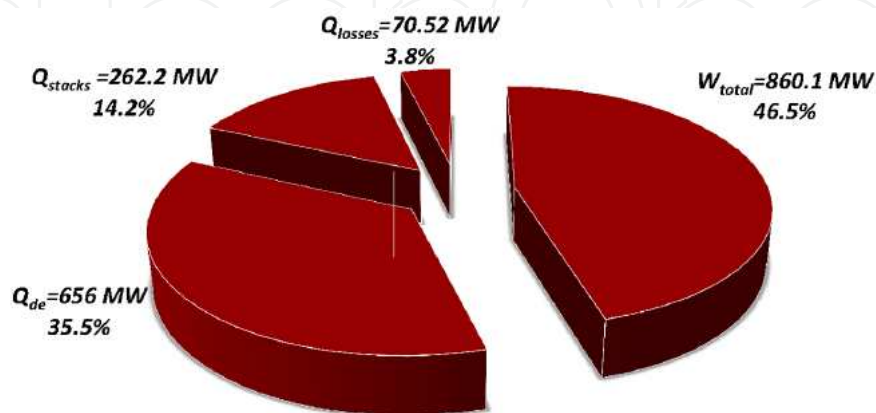


Figure 28. Energy balance of the given GTCC and MSF units (see online version for colors)

Q_{stack} is the largest heat loss and is accounted for about 14 % of the heat input.

The high stack temperature (183 °C) is due to the high feedwater temperature returning back from the MSF desalting units at 142 °C.

If GTCC is chosen without desalting plant, lower feedwater temperature is chosen and the stack temperature when NG without sulfur content was used; T_{stack} could be in the order of 100 °C.

5. Exergy analysis

An exergy analysis, based on the second law of thermodynamics, is conducted here for the cases considered before.

5.1. Compressor

The exergy destruction (irreversibility) in the compressor can be presented as follows:

$$I_{\text{comp}} = W_{\text{comp}} - A_{\text{comp}}$$

where A_{comp} is the increase of flow availability in the air stream across the compressor and equal to

$$A_{\text{comp}} = m_a \times [(h_2 - h_1) - T_e(s_2 - s_1)]$$

The second law efficiency of the compressor is expressed as

$$\varepsilon_{\text{comp}} = \frac{A_{\text{comp}}}{W_{\text{comp}}}$$

5.2. Combustion Chamber (cc)

The main exergy loss (or destruction) of the GT cycle occurs in the combustion chamber (cc) of the GT cycle. An exergy balance in the combustion chamber gives $E_f = E_3 - E_2 + I_{\text{cc}}$

The E_f , E_2 , E_3 , and i_{cc} are the exergies of fuel input, compressed air inlet, combusted gas exit, and exergy destructed (irreversibility), respectively.

E_f is almost equal to the mass fuel flow \times high heating value (HHV), HHV = 55,530 kJ/kg

For each GT, the value of $(E_3 - E_2)$ can be approximated by

$$E_3 - E_2 = m_g \times \frac{[(h_3 - h_2) - T_e(s_3 - s_2)]}{1000} = 426.196 \text{ MW}$$

Thus, the exergy destruction I_{cc} and combustion chamber second law efficiency ϵ_{cc} are calculated as

$$I_{cc} = E_f - (E_3 - E_2) = 716.17 - 426.19 = 290 \text{ MW}$$

$$\epsilon_{cc} = \text{Exergy gain/Exergy input} = 426.19/716.17 = 0.595$$

This is much lower than the combustion chamber energy efficiency, η_{cc} based on the thermodynamics first law and is usually assumed equal to 0.99.

5.3. Gas turbine

An exergy balance around the GT cycle gives

$$E_1 + E_f = E_4 + W_{GT} + I_{GT}$$

E_1 and E_4 are the exergy of air inlet to and gases leaving from the GT, respectively, and I_{GT} is the exergy destruction in the GT cycle. The values of these terms are calculated as

$$E_{4-1} = m_g \times [(h_4 - h_1) - T_e(s_4 - s_1)] / 1000 = 159.244 \text{ MW}$$

Since $W_{GT} = 215 \text{ MW}$, the exergy destruction in the GT cycle is

$$I_{GT} = E_f - (E_4 - E_1) - (W_{GT}) = 341.4 \text{ MW}.$$

This I_{GT} (341.4 MW) includes the energy destruction in the combustion chamber ($I_{cc} = 290 \text{ MW}$) and the balance = 51.4 MW is the exergy destruction in the cycle components, other than the combustion process.

The exergy difference utilized to produce the W_{GT} is $(E_3 - E_4) = 241.5 \text{ MW}$.

For the three GTs, this exergy difference is $3 \times 241.5 = 724.5 \text{ MW}$.

So, the effectiveness of the GT, ε_{GT} (without combustion chamber losses), is

$$\varepsilon_{GT}(\text{without combustion energy losses}) = 215/241.5 = 0.89$$

and the exergy destruction in the turbine, compressor due to friction is

$$I_{fric} = E_3 - E_4 - W_{GT} = (241.5 - 215) = 26.5 \text{ MW.}$$

The effectiveness of the GT cycle, when used as simple GT cycle is

$$\varepsilon_{GT}(\text{total}) = W_{GT}/E_f = 215/716.17 = 0.3 \text{ which is the same with gross efficiency based on HHV.}$$

When GTCC is used, the exergy of the exhaust gases E_4 is utilized to generate steam and operate steam turbine, and ε_{GT} in a GTCC is

$$\varepsilon_{GT}(\text{in GTCC}) = \frac{W_{GT} + (E_4 - E_1)}{E_f} = \frac{215 + 159.2}{716.17} = 0.523$$

5.4. Heat Recovery Steam Generator (HRSG)

In heat recovery steam generator (HRSG), the heat of hot gases leaving the GT is transferred to feedwater in deaerator, economizer, evaporator, and superheater and the heat transfer in the HRSG.

An exergy balance around the HRSG gives

$$\Delta E_g = \Delta E_w + I_{HRSG}$$

where ΔE_g is the exergy loss by the hot gases which is equal to the exergy gain by the water ΔE_w plus exergy destruction in one HRSG, I_{HRSG}

$$\Delta E_g = m_g \times [(C_p \times (T_4 - T_{stack}) - T_e (s_4 - s_{stack}))] = 129.108 \text{ MW}$$

$$\Delta E_w = m_w \times [(h_s - h_f) - T_e (s_s - s_f)] = 116.438 \text{ MW}$$

Then, $I_{HRSG} = (\Delta E_g - \Delta E_w) = 12.67 \text{ MW}$, and the effectiveness of HRSG is $\varepsilon_{HRSG} = \frac{\Delta E_w}{\Delta E_g} = 0.9$

So, the exergy difference gained by water in 3 HRSG = $3 \times 116.438 = 349.314 \text{ MW}$, and this is the exergy input to the steam cycle including the three MSF units.

5.5. Steam turbine cycle

The exergy difference across the ST cycle, ΔE_{ST} , is equal to $(E_{si} - E_{se})$, where E_{si} and E_{se} are the exergy of the steam inlet to the turbine and steam outlet to the MSF units, respectively.

$$\begin{aligned}\Delta E_{ST} &= 3 \times m_s \times \left[(h_{si} - h_{se}) - T_e (s_{si} - s_{se}) \right] = \\ &= 3 \times 97.86 \times \left[(3550.7 - 2781.5) - 323(6.95 - 7.2) \right] / 1000 = 249.531 \text{ MW}\end{aligned}$$

where s_{si} and s_{se} are the specific entropy of steam at the turbine inlet and outlet, respectively.

Then the exergy loss in the ST is

$$I_{ST}(\text{loss}) = \Delta E_{ST} - W_{ST} = 249.531 - 215.1 = 34.431 \text{ MW}$$

5.6. Desalination system

The exergy difference between the discharged steams from the turbine to the condensate from the brine heaters of one MSF unit, ΔE_{de} is as follows:

$$\begin{aligned}\Delta E_{de} &= m_{sd} \times \left[(h_{d,in} - h_{d,e}) - T_e (s_{d,in} - s_{d,e}) \right] = \\ &= 97.86 \times \left[(2783.5 - 496) - \frac{323(7.2 - 1.52)}{1000} \right] = 39.34 \text{ MW}\end{aligned}$$

where m_{sd} and $(h_{d,in} - h_{d,e})$, $s_{d,in}$ and $s_{d,e}$ are the steam flow rate to each MSF desalting unit, its specific enthalpy difference between the steam inlet, and its condensate exit from the desalting unit, specific entropy at steam inlet, and specific entropy of its condensate at the exit, respectively.

So, an exergy balance of the given CPDP using GTCC and MSF units shows that there are unaccounted losses due to steam extracted at moderately high pressure to operate the steam ejectors of the MSF units, and others and can be calculated as follows:

$$\begin{aligned}E_{unacct.} &= E_{f(\text{total})} - W_{GT(\text{total})} - \Delta E_{GT(\text{total})} - \Delta E_{HRSG(\text{total})} - W_{ST} - \Delta E_{de(\text{total})} - DE_{ST} - E_{rej} \quad (50) \\ E_{unacct.} &= 2148.5 - 646.5 - 1024.2 - 38 - 215.7 - 134.56 - 33.83 - 38.85 = 16.85 \text{ MW}\end{aligned}$$

5.7. Exergy distribution of the overall GTCC

Exergy balance of the given CPDP using GTCC and MSF units is conducted for the whole GTCC cycle.

The fuel exergy of the fuel supplied for the three GTs is

$$E_{f(\text{total})} = 3 \times m_f \times \text{HHV} = 2148.5 \text{ MW}$$

This fuel exergy is used to produce the power output power from the three GT= $3 \times 215 = 646.5$ MW.

So, the exergy loss from the GT cycles is

$$\Delta E_{GT(\text{total})} = 3 \times I_{GT} = 3 \times 341.4 = 1024.2 \text{ MW}$$

The exergy destruction in the three HRSG can be calculated as follows:

$$\Delta E_{HRSG(\text{total})} = 3 \times I_{HRSG} = 3 \times 12.67 = 38 \text{ MW}$$

The fuel exergy is utilized to produce output power from the steam turbine is

$$W_{ST} = 1 \times 215.7 = 215.7 \text{ MW}$$

The fuel exergy used to produce 45 MIGD from 3 MSF units is

$$\Delta E_{de(\text{total})} = 3 \times \Delta E_{de} = 3 \times 39.34 = 134.56 \text{ MW}$$

The exergy destruction in the steam turbine is $I_{ST} = 33.83 \text{ MW}$ and exergy loss to environment through the HRSG stacks can be calculated as follows:

$$\begin{aligned} E_{rej} &= 3 \times m_g \times \left[\frac{(h_{stuck} - h_1) - T_1(S_{stuck} - S_1)}{1000} \right] = \\ &= 3 \times 591.3 \times \left[\frac{(458.1 - 323.6) - 323(6.125 - 5.776)}{1000} \right] = 38.85 \text{ MW} \end{aligned}$$

There are unaccounted losses due to steam extracted at moderately high pressure to operate the steam ejectors of the MSF units, and others and can be calculated as follows:

$$\begin{aligned} E_{unacct.} &= E_{f(\text{total})} - W_{GT(\text{total})} - \Delta E_{GT(\text{total})} - \Delta E_{HRSG(\text{total})} - W_{ST} - \Delta E_{de(\text{total})} - DE_{ST} - E_{rej} \\ &= 2148.5 - 646.5 - 1024.2 - 38 - 215.7 - 134.56 - 33.83 - 38.85 = 16.85 \text{ MW} \end{aligned}$$

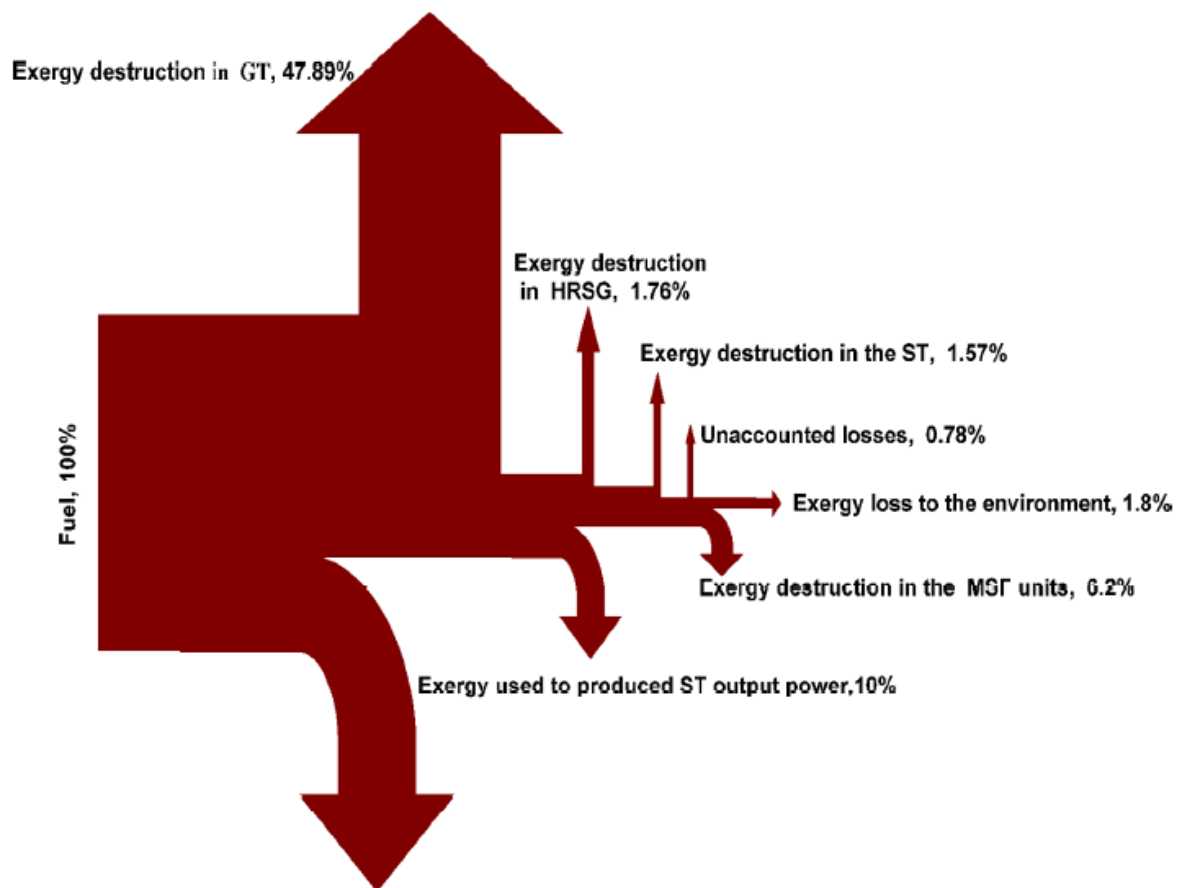


Figure 29. Grassmann diagram of the GTCC system (see online version for colors)

6. Fuel allocation between the EP and DW production

There are two methods to allocate the fuel between the EP and DW production, while the second is exergy method.

6.1. Work loss method

The first method is the work loss method. As mentioned, there is work loss due to discharging steam to the MSF units instead of its expansion to the condensing turbine. The CPDP outputs are

$3 W_{GT} = 646.5$ MW by the three GT, $W_{ST} = 215.7$ MW by steam turbine, and thermal energy input to the 3 MSFs, $3Q_{de} = 3 \times 218.68 = 656$ MW. It was showed that $3Q_{de}$ causes the loss (or equivalent to) $3 W_{de} = 136.34$ MW. The MSF units consume pumping energy at the rate of $W_{(pumping)} = 34.1$ MW, which should be deducted from the total power output.

So, the fuel charged to desalination to the total fuel supply should be

$$\begin{aligned} \text{Fuel}_{\text{energy to desal.}} &= \left(\frac{W_{\text{pumping}} + 3W_{de}}{3W_{GT} + W_{ST} + 3W_{de}} \right) \times Q_f = \\ &= \left(\frac{34.1 + 136.34}{646.5 + 215.7 + 136.34} \right) \times 1847.1 = 304.77 \text{ MW} \end{aligned}$$

The specific fuel energy charged to produce 1 m³ can be calculated as follows:

$$\text{Specific}_{\text{fuel energy to desal.}} = \left(\frac{\text{Fuel}_{\text{energy to desal.}} \times 24 \times 60 \times 60}{45 \text{ MIGD} \times 4550 \left(\frac{m^3}{\text{day}} \right)} \right) = 128 \frac{MJ}{m^3}$$

The fuel charged to produce the net power output can be calculated as

$$\text{Fuel}_{\text{energy to power}} = Q_f - \text{Fuel}_{\text{energy to desal.}} = 1847.1 - 304.77 = 1542.3 \text{ MW}$$

6.2. Exergy method

The aim of combining the 3 MSF units with the GTCC is to supply these units with its heat needs, $3 Q_{de} = 3 \times 218.68 = 656 \text{ MW}$. The exergy difference across the three MSF units is $3 \Delta E_{de} = 134.56 \text{ MW}$ and represents the exergy consumed by the desalting system.

The pumping work $W_{(\text{pumping})} = 34.1 \text{ MW}$ and work loss due to extraction of steam to the MSF steam ejector (2.4925 MW) should be added to $3 \Delta E_{de}$ to become 171.15 MW

This almost the same work was charged to the desalting units in the method of lost work, and there is no need to repeat the share of desalting in the fuel energy again.

It is clear that both methods give very close results, but the first method is easier and understandable by practitioner engineers.

6.3. Desalinated water cost

Since all combined cycle power plants in Kuwait were dual fuel (i.e., can be operated either by natural gas or heavy oil), the cost of desalinated water is evaluated in this section based on the current oil and natural gas prices. Hence, the desalinated water produced by this plant will be estimated based on two different types of fuel as follows:

The oil price is 60 \$/bbl and the low heating value of the oil is $LHV_{\text{oil}} = 42229 \text{ kJ/kg}$; so, the energy content in 1 barrel of oil (density of 900 kg/m^3) can be calculated as follows:

$$1 \text{ barrel} = 0.159 \text{ m}^3 \times 900 \frac{\text{kg}}{\text{m}^3} \times 42229 \frac{\text{kJ}}{\text{kg}} = 6.04 \text{ GJ}; \text{ so, the oil price per GJ will be } \$9.33/\text{GJ}$$

$$\text{The desalinated water cost} = \text{Specific}_{\text{fuel energy to desal.}} \frac{\text{GJ}}{\text{m}^3} \times \text{fuel price} \frac{\$}{\text{GJ}}$$

$$\text{The desalinated water cost} = 0.128 \frac{\text{GJ}}{\text{m}^3} \times 9.33 \frac{\$}{\text{GJ}} = 1.272 \frac{\$}{\text{m}^3}$$

When the gas price is \$2/MMBTU which is equivalent to 1.895 \$/GJ and $\text{LHV}_{\text{NG}} = 47806 \text{ kJ/kg}$.

$$\text{The desalinated water cost} = 0.128 \frac{\text{GJ}}{\text{m}^3} \times 1.895 \frac{\$}{\text{GJ}} = 0.243 \frac{\$}{\text{m}^3}$$

The following assumption is assumed for the analysis: steady state operation.

7. Sensitivity analysis

The developed equations were used to evaluate the performance of the reference CPDP using the GTCC in this section. A simplified schematic diagram of plant is shown in Figure 30, while state point conditions of the model are given in Table 5.

The model was tested against the available data of Al-Shuaiba CCPP, and the results showed good agreements as shown in Table 4. This model can also be used for simulation and/or parametric studies of the plants in order to evaluate its performance. A sensitivity analysis is carried out to investigate the effects of some combined cycle parameters on the overall efficiency, specific fuel energy to desalination, as well as the desalinated water cost. The selected parameters are ambient air temperature, compression ratio, and air-to-fuel ratio, turbine inlet temperature, and stuck temperature.

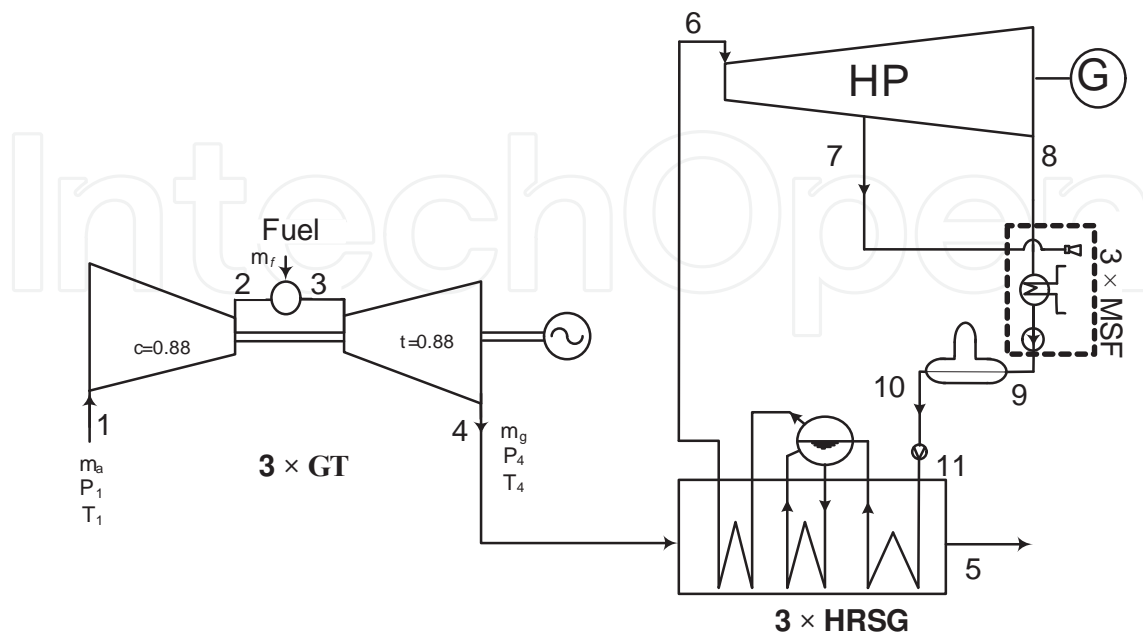


Figure 30. A simplified schematic diagram of Al-Shuaiba combined cycle power plant model

Point	Mass, kg/s	Pressure, Bar	Temp. °C	Enthalpy, kJ/kg	Entropy, kJ/kg	Exergy, kJ/kg
1	578.4	1.013	50	323.6	5.776	-1398
2	578.4	17.73	478.4	768.9	5.827	-967.6
3	591.3	17.73	1297	1720	6.678	-269.6
4	591.3	1.013	625	930.8	6.845	-1109
5	3 × 591.3	1.013	183	458.1	6.125	-1367
6	293.58	75	560	3520	6.941	1481
7	3 × 2.5	30.3	449.3	3342	7.076	1233
8	286.08	2.8	158.8	2781	7.155	648.4
9	293.58	13	118	495.4	1.503	47.39
10	293.58	6.8	142.3	598.7	1.761	73.81
11	293.58	87.2	142.3	603.9	1.753	81.5

Table 5. State point conditions of the model

Model	Actual	Operating and design conditions
		Gas turbine, 3 GT
578.62	578.62	Air mass flow rate, kg/s
44.86	44.86	Air-to-fuel ratio, A:F
17.5	NA	Pressure ratio, r_p
1297	NA	Turbine inlet temperature, °C
625	625	Exhaust gas temperature, °C
88.3	NA	Compressor isentropic efficiency, %
85	NA	Turbine isentropic efficiency, %
215.6	215.5	Power output, MW
35	NA	Gas turbine cycle efficiency, %
		Steam turbine, 1 ST
293.58	293.58	Steam mass flow rate, kg/s
75	75	High turbine inlet pressure, bar
560	560	High turbine inlet temperature, °C
2.8	2.8	Inlet pressure to MSF, bar
158.8	158.8	Inlet temperature to MSF, °C
215.5	215.7	Power output, MW
24.88	NA	Steam turbine cycle efficiency, %
		Heat recovery steam generator, 3 HRSG
6.8	6.8	Feedwater pressure, bar
142.6	142.3	Feedwater temperature, °C
20	20	Pinch point temperature difference, °C
183	183.1	Stack temperature, °C
		Desalination unit, 3 MSF
8.06	8	Gain ratio

Model	Actual	Operating and design conditions
789	789	Distillate output, kg/s
2.5	2.5	Inlet pressure to MSF, bar
135	135	Inlet temperature to MSF °C
2.5	2.5	Steam flow rate to ejector, kg/s
30	30	Inlet pressure to ejector, bar
450	449.3	Inlet temperature to ejector, °C
		GTCC
46.66	46.7	Combined cycle efficiency, %

Table 6. Mathematical model results against actual plant

The effect of ambient air temperature on the fuel allocation between the electric power and desalinated seawater production is presented in Figure 31. It shows that as the ambient air temperature increases, the allocated fuel to the electric power decreases, and this led to increase the allocated fuel to desalination. Figure 32 shows the effect of ambient temperature on the combined cycle efficiency at different compression ratios. It is clear that the cycle efficiency is the highest at maximum pressure ratio and minimum ambient temperature. On the other hand, the effect of air-to-fuel ratio is limited as shown in Figure 33.

Figure 34 shows the effect of ambient and turbine inlet temperatures (TIT) on the specific fuel energy to desalination. It shows that the specific fuel energy to desalination increases at high ambient temperatures, while it decreases at higher turbine inlet temperatures.

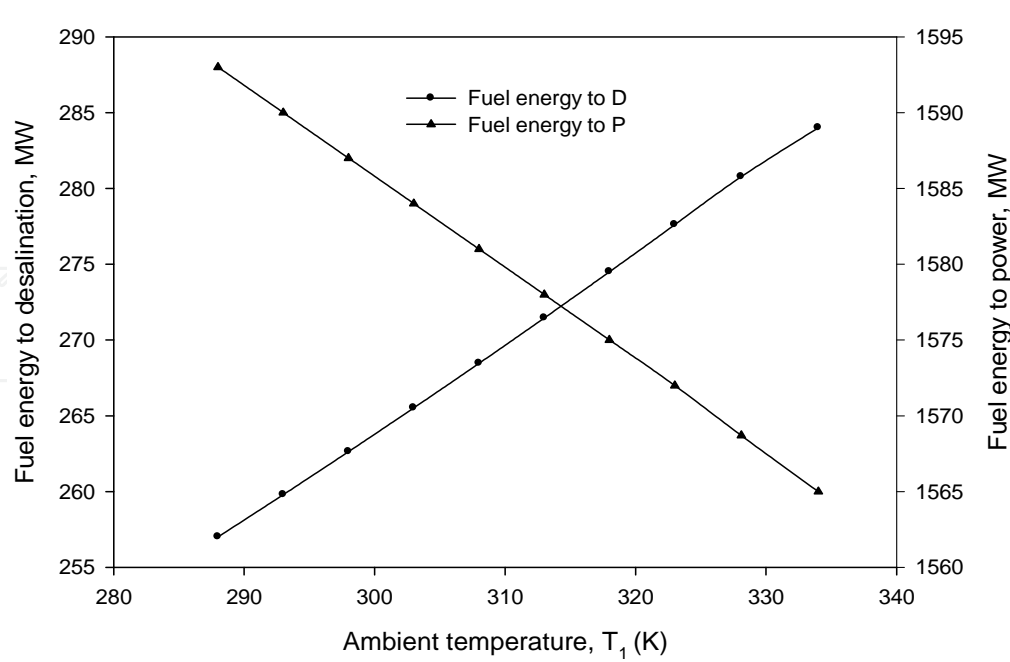


Figure 31. The effect of air ambient temperature to fuel allocation between the electric power and desalinated seawater production

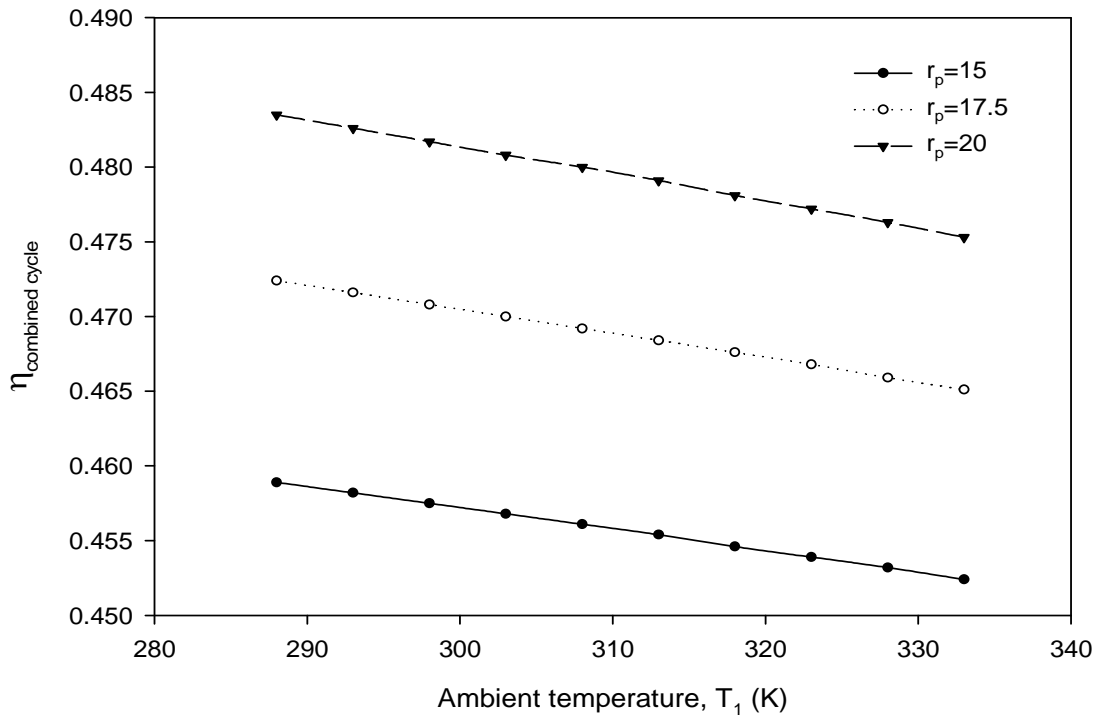


Figure 32. The effect of ambient temperature on the combined cycle efficiency at different compression ratios

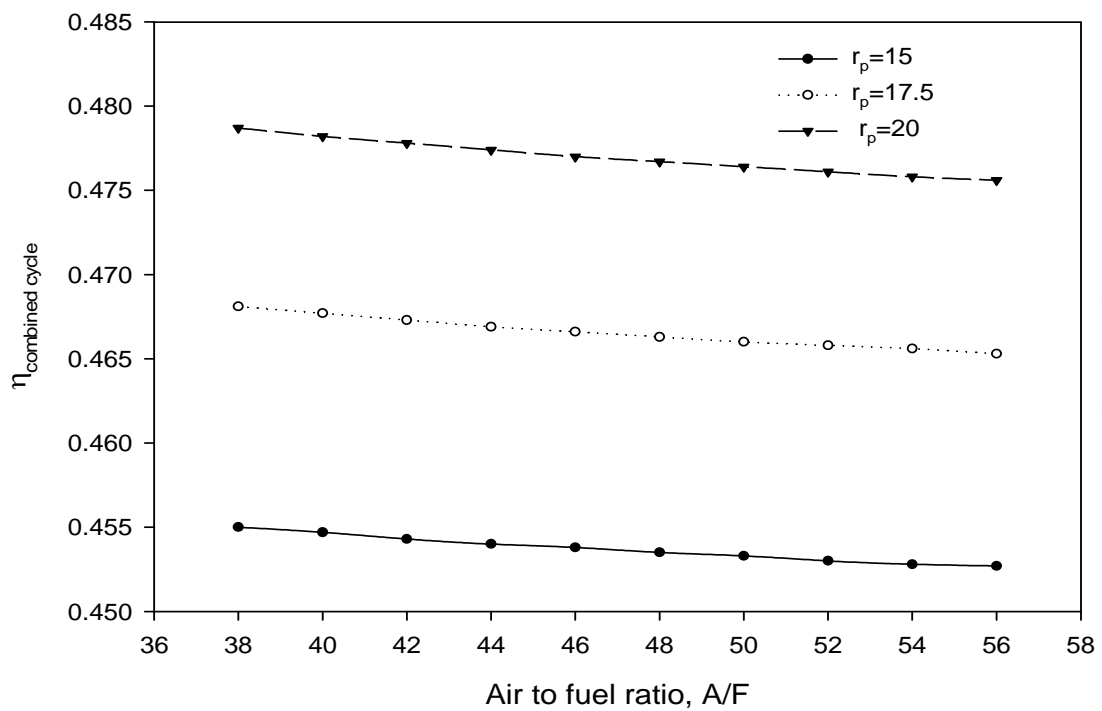


Figure 33. The effect of air-to-fuel ratio on the combined cycle efficiency at different compression ratios

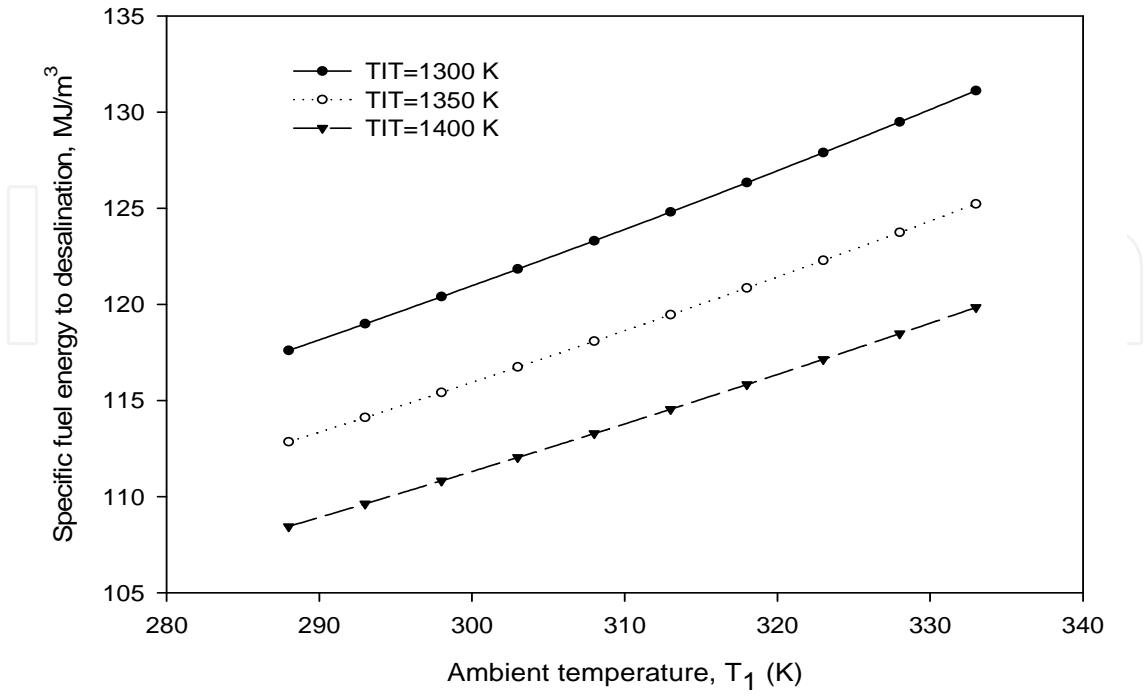


Figure 34. The effect of ambient temperature on the specific fuel energy to desalination at different turbine inlet temperatures

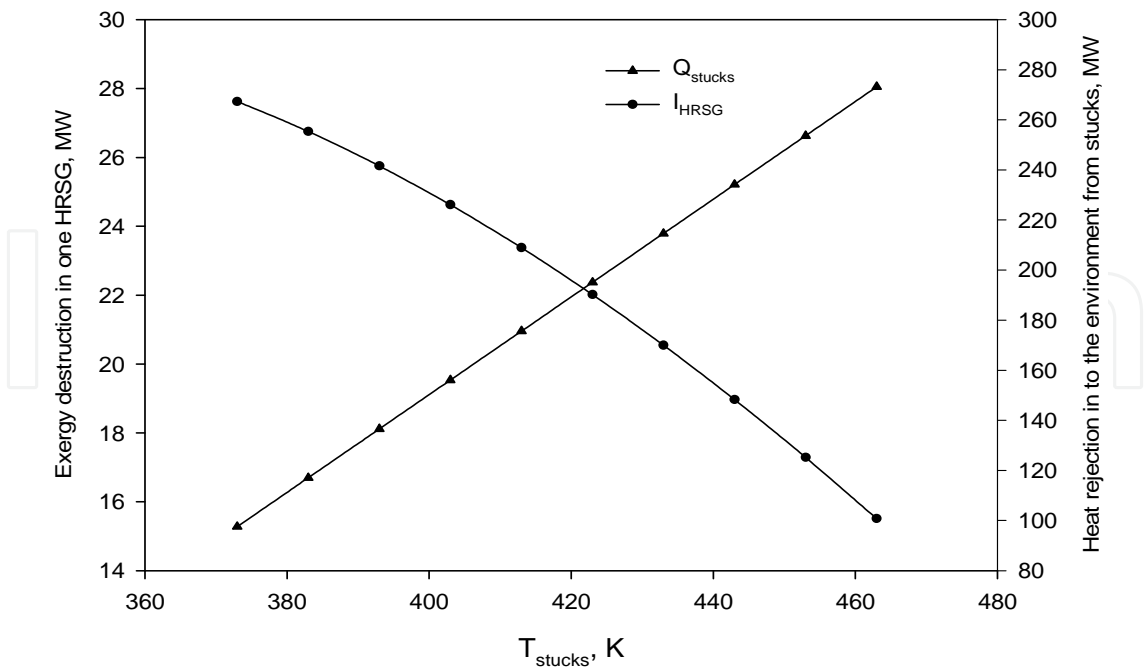


Figure 35. The effect of stack temperatures on the heat rejection into environment as well as on the HRSG exergy destruction

On the other hand, the effect of stack temperatures on the heat rejection into environment as well as on the exergy destruction of HRSG is depicted in Figure 35. It is clear that as the stack temperatures increases, the heat rejection into the environment will increase and consequently the exergy destruction in HRSG will decrease.

The main real problem by this plant is the high stack temperature of 183 °C because the high feedwater returns from the MSF desalting units at 135 °C. If the stack temperature is reduced to 110 °C, the heat gained by the water in the HRSG temperature is increased to 16.5 %, and the ST output would increase to 251.32 MW. The difference between this ST output and actual output of 215.7 by the ST or 35.62 should be charged as well to the desalting process. Again for net efficiency of 44 %, the fuel energy of 80.955 MW should be added to the 188.8 MW calculated before, or the fuel charged for thermal energy would be 269.75 or 113 MJ/m³.

Although the effect of steam turbine inlet pressure on the specific fuel energy to desalination is negligible, it will slightly be affected by the types of fuel as shown in Figure 37.

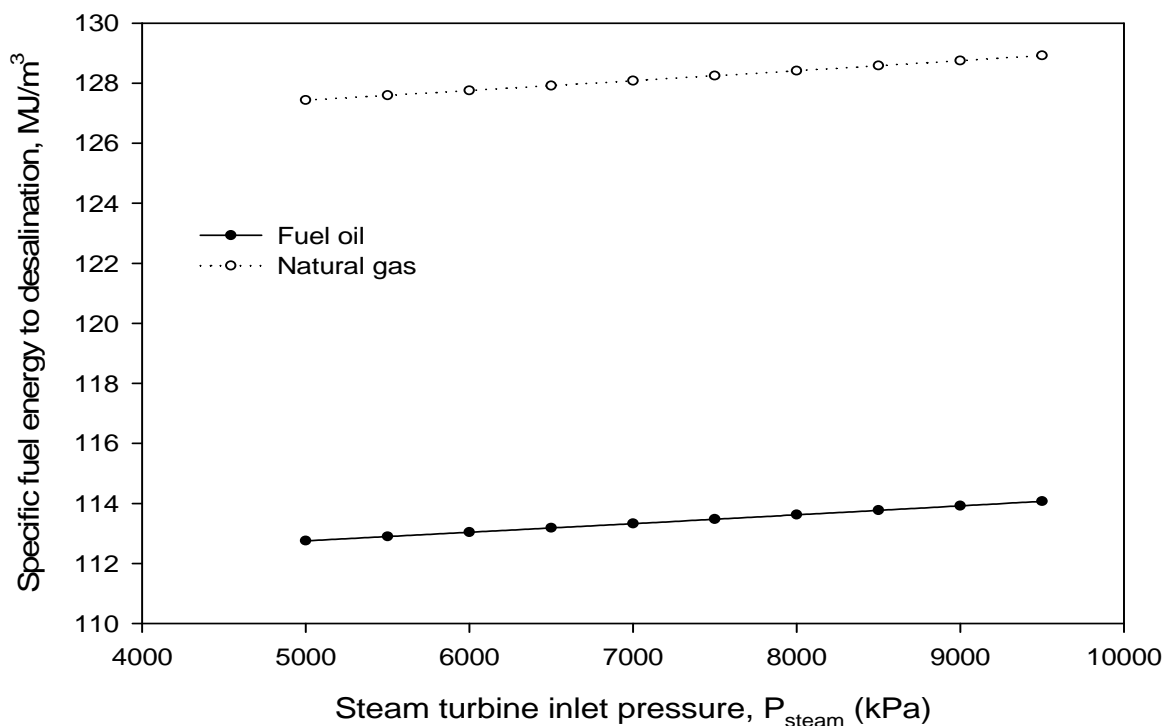


Figure 36. The effect of steam turbine inlet pressure on the specific fuel energy to desalination at different types of fuel

Figure 38 shows the effect of ambient temperature on the specific fuel energy to desalination when different types of fuel are used. Since there is a large difference in price per unit of energy between oil and natural gas, the cost of desalinated water is strongly affected by the fuel type as shown in Figure 39.

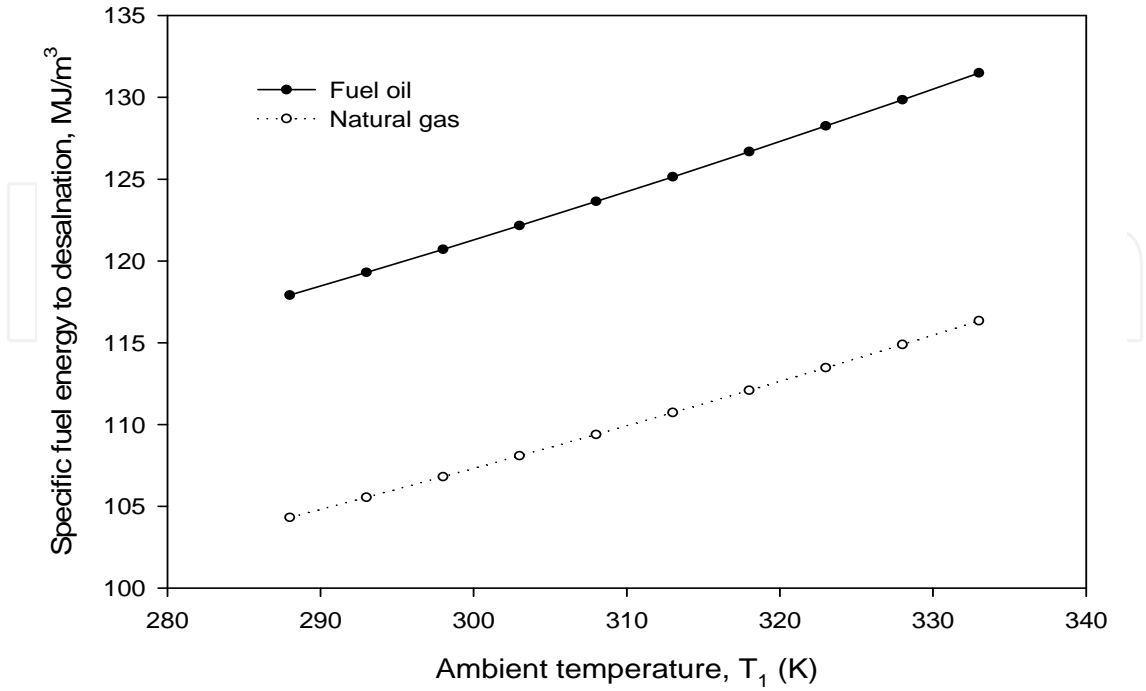


Figure 37. The effect of ambient temperature on the specific fuel energy to desalination at different types of fuel

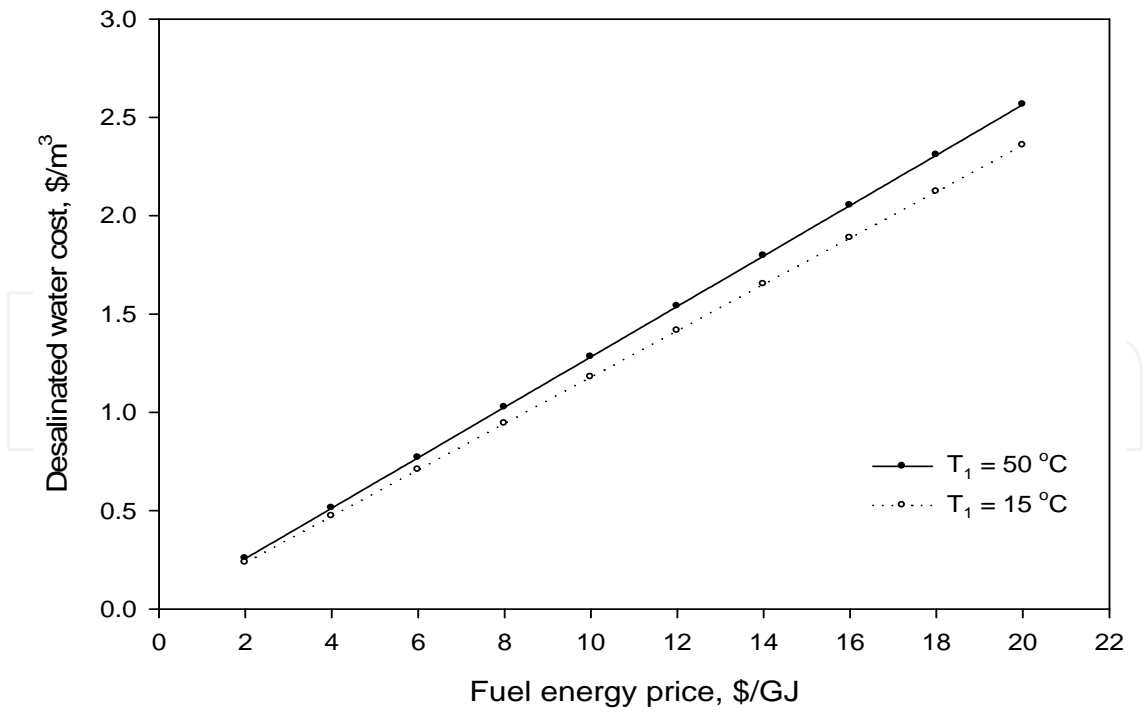


Figure 38. The effect of fuel energy price on the desalinated water cost at different ambient temperatures

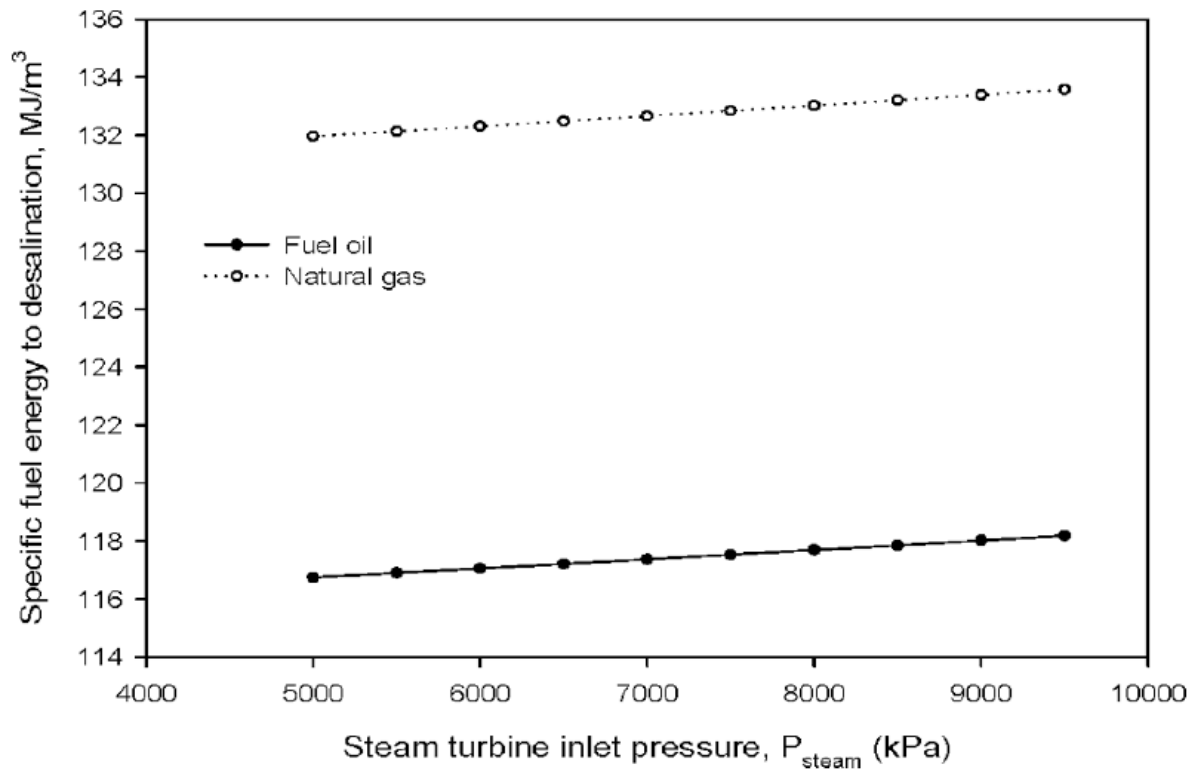


Figure 39. The effect of steam turbine inlet pressure on the fuel energy allocated to DW at different types of fuel

8. Conclusion

A general overview on the CPDP using GTCC is presented including description and analysis of the GTCC component. Energy and exergy analyses, based on the first and second laws of thermodynamics, respectively, were conducted on CPDP using GTCC connected with MSF desalting system. The concept of work loss due to exhausting steam from the ST at higher pressure and temperatures compared to end condenser condition was introduced and calculated. The exergy at different points of both GT and ST cycles and HRSG and the exergy destructions in several components were calculated. The main exergy loss was found in the GT combustion chambers. The fuel energy allocation between the desalting process and power production was conducted, based on the work loss and exergy methods. Both methods gave almost the same results. The main problem detected from the design of the given plant the high stack temperature of 183 °C of the HRSG to match that of high feedwater returning from the MSF desalting units at 135 °C. In GTCC using condensing turbines and NG with no sulfur, the typical HRSG stack temperature is 100 °C. The decrease of the stack temperature is reduced from 183 °C to 100 °C, which would increase the heat gain by the HRSG and ST work output about 19 %. This means that ST work output would be 256.6 MW. The difference between this ST output and actual output of 215.7 by the ST or 40.9 MW should be charged to also to the

desalting process. Again, for net efficiency of 44 %, the fuel energy of 92.94 MW should be added to the 188.8 MW calculated before, or the fuel charged for thermal energy would be 281.82 MW or 119 MJ/m³.

Sensitivity analysis shows that the pressure ratio, inlet air temperature, turbine inlet temperature, and stack temperature have a significant role in the combined cycle performance. It shows also that the cost of desalinated water is strongly affected by the fuel type because there is a large difference in price per unit of energy between oil and natural gas.

Nomenclature

a	specific exergy, kJ/kg
A	stream availability, mass flow rate×specific exergy, kW or MJ
B	brine flow, kg/s
BH	brine heater
BPST	back pressure steam turbine
CPDP	cogeneration power-desalting plant
D	distillate output flow rate, kg/s or MIGD
DP	desalting plant
DW	desalted seawater
ECST	extraction condensing steam turbine
EP	electric power
F	seawater feed flow rate, kg/s
FH	feed heater
GCC	Gulf Cooperation Countries
GR	gain ratio, distillate D per heating steam S, D:S
GT	gas turbine
GTCC	gas-steam turbine combined cycle
h	specific enthalpy, kJ/kg
H	heat rate (3,600/h), kJ/kWh
HHV	fuel high heating value, kJ/kg
HP	high pressure
HRSG	heat recovery steam generator
IP	intermediate pressure
kWh	3,600 kJ/s
L	latent heat of vaporization, kJ/kg

LHV	fuel low heating value, kJ/kg
LP	low pressure
m	mass flow rate, kg/s
MED	multi-effect distillation system
ME-TVC	multi-effect thermal vapor compression desalting system
MIGD	million imperial gallons per day (4,546 m ³ /day or 52.616 kg/s)
MSF	multistage flash desalination
MVC	mechanical vapor compression desalting system
MW	megawatts
net	net output
P	pressure, kPa or bar
PP	power plant
PR	performance ratio, kg of distillate/2,330 kJ of heat
Q	rate of heat addition or rejection
RO	reverse osmosis
Sd	steam supply to desalting plant
SG	steam generator
SPD	single-purpose desalting plant
SPP	separate power plant
ST	steam turbine
SWRO	seawater reverse osmosis
TC	thermal compressor
TTD	terminal temperature difference
TVC	thermal vapor compression desalting system
v	specific volume, m ³ /kg
W	power output
W _{cp}	cycle work
W _d	equivalent work of heat supply to desalting units
W _{np}	net power output
W _p	pumping work of desalting unit

Greek letters

ϵ	second law efficiency or effectiveness
η_b	boiler efficiency
η_{is}	isentropic efficiency of pump or turbine

Subscripts

b	boiler or brine
bd	blowdown stream
cw	cooling seawater
d	desalting unit, discharge vapor, or distillate
e	extracted steam
e	environment
f	saturated liquid properties, feed heaters, or fuel
g	saturated vapor properties
pp	power plant
r	reheat

Author details

M.A. Darwish, H.K. Abdulrahim*, A.A. Mabrouk and A.S. Hassan

*Address all correspondence to: habdelrehem@qf.org.qa

Qatar Environment and Energy Research Institute, Qatar Foundation, Doha, Qatar

References

- [1] Mohamed A. Darwish, Hassan K. Abdulrahim, Anwar B. Amer, On better utilization of gas turbines in Kuwait, *Energy* 33 (2008) 571–588
- [2] John Xia, Rick Antos, (W501F) 3 Million hours fleet operational experience, POWER-GEN International 2006 – Orlando, FL, November 28-30, 2006, http://www.energy.siemens.com/co/pool/hq/energy-topics/pdfs/en/gas-turbines-power-plants/9_SGT65000F.pdf
- [3] Armin Städtler, Meeting the Middle East Energy Demand with the Proven 8000H Series, Power-Gen Middle East, Abu Dhabi, 2014-10-12, http://www.energy.siemens.com/nl/pool/hq/energy-topics/technical-papers/2014-10-12_PGME_8000H.pdf
- [4] Olav Bolland, Thermal power Generation, (2014), http://folk.ntnu.no/obolland/pdf/kompendium_power_Bolland.pdf

- [5] Bob Shepard, Gas turbines technologies for electric generation, Power Plant Primer - Combustion Turbines - IEEE Mississippi Section, <http://www.ieeems.org/Meetings/presentations/MS3-ASME%20Gas%20Turbine%20Technologies%20Presentation.ppt>
- [6] LM2500+ Aeroderivative Gas Turbine Package (29 MW), <https://www.ge-distributed-power.com/products/power-generation/15-to-35-mw/lm2500>
- [7] Magdalena Milancej, Advanced Gas Turbine Cycles: Thermodynamic Study on the Concept of Intercooled Compression Process, Diploma thesis, Institut für Thermodynamik und Energiewandlung Technische Universität Wien and Institute of Turbomachinery, Technical University of Lodz, http://publik.tuwien.ac.at/files/pubmb_3689.pdf
- [8] Ivan Sigfrid, Investigation of a prototype industrial gas turbine combustor using alternative gaseous fuels, Ph. D. Thesis, Division of Thermal Power Engineering, <http://lup.lub.lu.se/luur/download?func=downloadFile&recordOId=3972178&fileOId=3972217>
- [9] Turbine Inlet Air Cooling, From Wikipedia, the free encyclopedia, http://en.wikipedia.org/wiki/Turbine_Inlet_Air_Cooling
- [10] Frank J. Brooks, GE gas turbine performance characteristics, <http://www.muellerenvironmental.com/Documents/GER3567H>
- [11] Bob Omidvar, Gas Turbine Inlet Air Cooling System, http://www.albadronline.com/oldsite/books/49_GasTurbineInlet.pdf
- [12] Gas turbine inlet air fogging, <http://www.meefog.com/wp-content/uploads/br-gt-gasturbine.pdf>
- [13] Claire M. Soares, Gas turbines in simple cycle and combined cycle applications, <http://www.netl.doe.gov/File%20Library/Research/Coal/energy%20systems/turbines/handbook/1-1.pdf>
- [14] Multistage Axial Compressors, section 12.4, <http://web.mit.edu/16.unified/www/FALL/thermodynamics/notes/node92.html>
- [15] Ernesto Benini (2010). Advances in Aerodynamic Design of Gas Turbines Compressors, Gas Turbines, Gurrappa Injeti (Ed.), ISBN: 978-953-307-146-6, InTech, Available from: <http://www.intechopen.com/books/gas-turbines/advances-in-aerodynamic-design-of-gas-turbines-compressors>
- [16] Scott Samuelsen, Conventional Type Combustion, <http://www.netl.doe.gov/File%20Library/Research/Coal/energy%20systems/turbines/handbook/3-2-1-1.pdf>
- [17] The Jet Engine, Rolls Royce, ISBN 0 902121 2 35, <http://www.amazon.com/The-Jet-Engine-Rolls-Royce/dp/0902121049>
- [18] Mohammad Nazri Mohd. Jaafar, Azeman Mustafa, Madya Hamidon Musa, Wan zaidi Wan Omar, Mohd. Zamri Yusoff, Kamsani Abdul Majid, Mohamad Shaiful Ashrul

- Ishak, Development of low NO_x liquid fuel burner, Faculty of Mechanical Engineering, Universiti Teknologi Malaysia 2005, http://eprints.utm.my/539/1/LAPOR-AN_AKHIR_IRPA_74069.pdf
- [19] AP 42, Fifth Edition, Volume I, Chapter 3: Stationary Internal Combustion Sources, Stationary Gas Turbines, <http://www.epa.gov/ttn/chief/ap42/ch03/final/c03s01.pdf>
- [20] Ueli Honegger, Gas turbine combustion modeling for a parametric emissions monitoring system, M.Sc. thesis, Kansas State University, 2007, <https://krex.k-state.edu/dspace/bitstream/handle/2097/371/UeliHonegger2007.pdf?sequence=1>
- [21] Bassam G. Jabboury and Mohamed A. Darwish, Performance of gas turbine co-generation power desalting plants under varying operating conditions in Kuwait, Heat Recover), Systems & CHP Vol. 10, No. 3, pp. 243-253, 1990
- [22] Bassam G. Jabboury and Mohamed A. Darwish, The effect of the operating parameters of heat recovery steam generators on combined cycle/sea-water desalination plant performance, Heat Recover) Systems & CHP, Vol. 10, No. 3, pp. 255-267, 1990
- [23] J. Dastych, Pickhardt, H. Unbehauen, Control schemes of cogenerating power plants for desalination, in Process Instrumentation, Control and Automation, from Encyclopedia of Desalination and Water Resources, Eolss Publishers, Paris, France, [<http://www.desware.net>] [Retrieved January 5, 2015]
- [24] Steam turbine technology HEATs up, Power Engineering International, <http://www.powerengineeringint.com/articles/print/volume-11/issue-3/features/steam-turbine-technology-heats-up.html>
- [25] M. Boss, Steam turbines for STAG combined-cycle power systems, http://site.ge-energy.com/prod_serv/products/tech_docs/en/downloads/ger3582e.pdf
- [26] SSS CLUTCH, Key to combined cycle flexibility, http://www.sssclutch.com/power-generation/combinedcycle/attachments/NR9905_2.pdf
- [27] R.W. Smith, P. Polukort, C.E. Maslak, C.M. Jones, B.D. Gardiner, Advanced Technology Combined Cycles, http://site.ge-energy.com/prod_serv/products/tech_docs/en/downloads/ger3936a.pdf
- [28] J.P. Ninan and B. Khan, SPECIAL DESIGN ASPECTS OF CO-GENERATION UNITS, in Thermal Power Plants and Co-generation Planning, from Encyclopedia of Desalination and Water Resources, Eolss Publishers, Paris, France, [<http://www.desware.net>] [Retrieved January 5, 2015]
- [29] G. Volpi, G. Silva, R. Piasente, Ansaldo Caldaie experience in HRSG design developments. <http://www.ansaldoboiler.it/prodotti/generatori-di-vapore-a-recupero/%3Faid%3D747%26sa%3D1>
- [30] M.A. Darwish, Anwar Bin Amer, Cost allocation in cogeneration power-desalination plant utilising gas/steam combined cycle (GTCC) in Kuwait, *Int. J. Exergy*, Vol. 14, No. 3, 2014 275